Characterization of *Caenorhabditis elegans* METL-13 during health and disease

Thesis for the degree of *Philosophiae Doctor*

by

Melanie Lianne Engelfriet

Department of Biosciences

Faculty of Mathematics and Natural Sciences

University of Oslo

2023

Series of dissertations submitted to the
Faculty of Mathematics and Natural Sciences, University of Oslo
No. 2716

ISSN 1501-7710

Cover: UiO.
Print production: Graphic center, University of Oslo.

Contents

Acknowledgements

I would not have been able to complete this journey without the help of numerous people. Therefore, I want to start with a collective **Thank you** – I have been very lucky to have your support.

Rafal – First and foremost, I want to thank my main supervisor, Rafal Ciosk. Thank you for giving me the opportunity to work in your group and for all the guidance over the past few years. You have always been available when I needed help, whether it be offering advice on projects and ideas or hair to cluster nematodes prior to imaging. You have inspired me to continue my scientific endeavor, to always be curious, and to watch The Red Green Show (which is a new favorite of mine now). I have truly enjoyed working together throughout my Ph.D. journey.

Pål – I am equally grateful to my co-supervisor, Pål Falnes, for allowing me to work on this project. Your extensive knowledge on methyltransferases is truly inspiring and has aided me greatly throughout this journey. Your door has always been open for any kind of discussion, which I have always appreciated.

Ciosk group – I have been very lucky to have worked in a group with so many great members, past and present. Firstly, I would like to acknowledge Frida, Benedicte, and Synne, whom I had the pleasure of sharing an office with. Frida**,** you are an amazing person inside and outside of the lab. Thank you for all the fun conversations, for enjoying the Eurovision Song Contest with me, but most importantly: Thank you for introducing us all to the concept of fika! Benedicte**,** I can never thank you enough for all the chunking and bleaching of my worms whenever Vy was being Vy. Thank you for always keeping this lab running smoothly, I know I am not the only one who appreciates you for this. And of course, thank you for always being there to discuss our drama TV shows. Synne**,** thank your making it feel a bit less lonely to come into the lab on the weekend.

It has been great to have you around and I am sure you will uncover great things during your doctoral journey. A special thanks to Pooja, Suman, Tina and Niladri, for your advice, help, or even just for all the conversations and laughs.

Falnes group – A huge thanks to the current and former members of this wonderful group! Jedrek, Carmen, Lisa, Erna, Kamilla, and Mads: thank you for your feedback on this project, the interesting discussions, and for all the fun on social outings.

Maciej – Thank you for being the best friend a person could ask for. I look forward to many more years of discussing why corkwing wrasse and nematodes are amazing.

Torbjørn – Thank you for always showing off how great of a cook you are on our Tuesdays after going to the gym. Whether I had a good or a bad day, you and Maciej were always there to raise a glass with me.

Alissa & Rick – Bedankt voor het altijd laten voelen alsof er geen dag is verstreken sinds mijn laatste bezoek. Het is altijd bizar hoe we elkaar een halfjaar niet zien en dan gewoon opeens samen zitten te breien alsof er niets is gebeurd. Ik kijk steeds uit naar de reünie van Greet & Gerda! En natuurlijk hoeveel lieve kleine Noa is gegroeid sinds de laatste keer (dat gaat steeds veel te snel). Jullie zijn altijd één van de grootste redenen zijn waarom ik met een glimlach op een KLM vlucht naar Nederland zit. Blijf altijd funnig!

Onsrud familien – Det har vært vanskelig å være borte fra familien min, men å være rundt Onsrud familien har fått alt å føles litt mer hjemmekoselig. Tusen takk for alle invitasjoner til ferier, bursdager eller bare små helgeturer. Spesiell takk til Maren, for alltid å åpne hjemmet sitt for meg. Og, selvfølgelig, takk til Mathias, som alltid fikk alle bekymringene mine til å flyte bort etter en dårlig dag. Du får meg alltid til å smile når jeg kommer hjem.

Mijn fantastische familie – Mam, pap, Anja, Joeri, en Jaimy, deze scriptie zou uiteraard nooit hebben bestaan zonder jullie. Dankjewel voor het steeds ophalen en brengen naar Schiphol, voor gezellig de hele dag door koffie drinken, en natuurlijk alle pakketjes die ik heb gekregen door de jaren heen. Ik had het nooit zo ver kunnen schoppen zonder jullie, en daarvoor ben ik jullie eeuwig dankbaar. Ik kijk er heel erg naar uit om de afsluiting van deze fase van mijn leven met jullie te vieren.

Summary

The addition of a methyl group (CH_3) to proteins on specific amino acids can influence their localization, interactions, or fine-tune their enzymatic activity. The methylation of proteins is mediated by a large group of specialized enzymes named methyltransferases. One such enzyme is methyltransferase-like protein 13 (METTL13), which functions as a dual methyltransferase responsible for methylating the eukaryotic elongation factor 1 alpha (eEF1A) protein at two distinct sites. In humans, it trimethylates the N-terminal glycine 2 ($eEF1A^{G2me3}$) and dimethylates lysine 55 ($eEF1A^{K55me2}$). This highly conserved factor is involved in the translation elongation step during protein synthesis, an essential cellular mechanism. Interestingly, both METTL13 and $eEF1A^{K55me2}$ are upregulated in a plethora of human cancers. The absence of either METTL13 or its downstream methylation mark $eEF1A^{K55me2}$ leads to reduced protein synthesis and cell proliferation in human cancer cell lines but appears not to affect non-transformed cell lines. This makes METTL13 an attractive target for cancer therapy. However, studies investigating the role of METTL13 have thus far been conducted in human cells and specific tissues in mice. Here, we used the nematode *Caenorhabditis elegans* as a model to study the function of METTL13 by assessing its loss in a whole-animal setting. We show that the biochemical function of METTL13 is conserved, as *C. elegans* METTL13 (METL-13) methylates eEF1A (EEF-1A) similarly to what has been described in humans. Importantly, the tumor-promoting role of METL-13 and $EEF\text{-}1A^{K55me2}$ is also conserved, with a lack of either resulting in phenotypically less severe germline tumors. Furthermore, METL-13 appears non-essential for animal development, growth, and stress responses. Our studies endorse targeting $eEF1A^{K55me2}$ for cancer therapy and introduce *C. elegans* as a METTL13-cancer model.

Sammendrag

Påsetting av metylgrupper (CH_3) på spesifikke aminosyrer i proteiner kan påvirke og regulere disses lokalisering, interaksjoner eller enzymatiske aktivitet. Metyleringen av proteiner katalyseres av en stor gruppe spesialiserte enzymer kalt metyltransferaser. Ett av disse enzymene er metyltransferase-like protein 13 (METTL13), som fungerer som en «dobbel» metyltransferase og er ansvarlig for metylering av proteinet «eukaryotic elongation factor 1 alpha» (eEF1A) på to forskjellige steder hos mennesker: trimetylering av den N-terminale glycin 2 ($eEF1A^{G2me3}$) og dimetylering av lysin 55 ($eEF1A^{K55me2}$). Denne svært konserverte faktoren er involvert i translasjon elongering under proteinsyntese, en essensiell cellulær mekanisme. Interessant nok er både METTL13 og $eEF1A^{K55me2}$ oppregulert i en rekke kreftformer hos mennesker. Fraværet av enten METTL13 eller $eEF1A^{K55me2}$ fører til redusert proteinsyntese og celleproliferasjon i humane kreftcellelinjer, men ser ikke ut til å påvirke ikke-transformerte cellelinjer. Dette gjør METTL13 til et attraktivt mål for kreftbehandling. Studier på rollen til METTL13 har bare blitt utført i humane celler og spesifikke organer hos mus. Vi brukte nematoden *Caenorhabditis elegans* som en modell for å bestemme funksjonen til METTL13, og studere effekten av fraværet av dette enzymet i en hel organisme. Vi viser at *C. elegans* METTL13 (METL-13) er ansvarlig for den samme metyleringen av eEF1A (EEF-1A) som beskrevet for mennesker. Den kreftfremmende rollen til METL-13 og $EEF\text{-}1A^{K55me2}$ ble også observert i nematoden, hvor fravær av disse resulterte i fenotypisk mindre alvorlige svulster i kimbanen. Videre fremstår METL-13 som ikke-essensiell for dyrs utvikling, vekst og stressresponser. Studiene våre understøtter mulig bruk av $eEF1A^{K55me2}$ rettet terapi i kreftbehandling og introduserer *C. elegans* som en modell for forskning på METTL13 i sammenheng med kreft.

Samenvatting

De toevoeging van een methyl groep (CH_3) aan eiwitten op specifieke aminozuren kan hun locatie en interacties beïnvloeden of enzymatische activiteit verfijnen. De methylatie van eiwitten wordt gemedieerd door een grote groep gespecialiseerde enzymen genaamd methyltransferases. Eén van deze enzymen is de methyltransferase-like eiwit 13 (METTL13), een duale methyltransferase dat verantwoordelijk is voor de methylatie van het eukaryote elongatiefactor 1 alfa (eEF1A) op twee verschillende plaatsen: de trimethylatie van glycine 2 ($eEF1A^{G2me3}$) en de dimethylatie van lysine 55 ($eEF1A^{K55me2}$). Deze sterk geconserveerde factor is betrokken bij de translatie elongatie stap tijdens eiwitsynthese, een essentieel cellulair mechanisme. Interessant genoeg zijn zowel METTL13 als $eEF1A^{K55me2}$ opgereguleerd in veel menselijke kankers. De afwezigheid van METTL13 of $eEF1A^{K55me2}$ leidt tot verminderde eiwitsynthese en cel proliferatie in menselijke kankercellijnen, maar lijkt niet-getransformeerde cellijnen niet te beïnvloeden. Dit maakt METTL13 een aantrekkelijk doelwit om kanker te bestrijden. Onderzoeken naar de rol van METTL13 zijn alleen uitgevoerd in menselijke cellen en specifieke organen van muizen. Wij hebben de nematode *Caenorhabditis elegans* als model gebruikt om de functie van METTL13 te achterhalen, waarbij wij het effect van de afwezigheid van dit enzym hebben bestudeerd in een heel organisme. We laten zien dat *C. elegans* METTL13 (METL-13) verantwoordelijk is voor dezelfde methylatie van eEF1A (EEF-1A), zoals voor mensen is beschreven. De tumor bevorderende rol van METL-13 en EEF-1AK55me2 is ook behouden in de nematode, waarbij het ontbreken van beide resulteert in fenotypisch minder ernstige kiemlijn tumoren. Ook lijkt METL-13 niet essentieel voor de ontwikkeling, groei en stressreacties van de nematode. Ons onderzoek ondersteunt $eEF1A^{K55me2}$ gerichte therapie voor kanker en introduceert *C. elegans* als een model vooronderzoek naar METTL13 in de context van kanker.

Abbreviations

7BS	–	Seven-beta-strand
aa-tRNA	–	Aminoacyl-tRNA
AdoHcy	–	*S*-adenosylhomocysteine
AdoMet	–	*S*-adenosylmethionine
C. elegans	–	*Caenorhabditis elegans*
CGC	–	*Caenorhabditis* Genetics Center
CH_3	–	Methyl group
CRISPR-Cas9	–	Clustered regularly interspaced palindromic repeats and CRISPR-associated protein 9
DIC	–	Differential interference contrast
E. coli	–	*Escherichia coli*
EEF-1A	–	Eukaryotic elongation factor 1 alpha in *C. elegans*
EEF-1A^{K55me2}	–	Dimethylated lysine 55 on EEF-1A
eEF1A	–	Eukaryotic elongation factor 1 alpha
eEF1A^{K55}	–	Lysine 55 on eEF1A
eEF1A^{K55me2}	–	Dimethylated lysine 55 on eEF1A
eEF1A^{G2me3}	–	Trimethylated glycine 2 on eEF1A
eEF1B	–	Eukaryotic elongation factor 1 beta
FEAT	–	Faint expression in normal tissues, aberrant overexpression in tumors
G2	–	Glycine at position 2
G2me3	–	Trimethylated glycine at position 2
GDP	–	Guanosine-5’-diphosphate
GFP	–	Green fluorescent protein
GTP	–	Guanosine-5’-triphosphate
H3K4	–	Lysine 4 on the tail of histone 3
H3K9	–	Lysine 9 on the tail of histone 3
K55	–	Lysine at position 55
K55me2	–	Dimethylated lysine at position 55
KDMT	–	Lysine demethylase

Kme0/1/2/3	–	Unmethylated, monomethylated, dimethylated, or trimethylated lysine
KMT	–	Lysine-specific methyltransferase
L1/2/3/4	–	Larval stage 1/2/3/4
METL-13	–	Methyltransferase-like protein 13 in *C. elegans*
METTL13	–	Methyltransferase-like protein 13
MS	–	Mass spectrometry
MT13-C/N	–	C/N- terminal MTase domain of METL-13
MTase	–	Methyltransferase
NBRP	–	National Bioresource Project
NGM	–	Nematode growth medium
NTMT	–	N-terminal methyltransferase
PDAC	–	Pancreatic ductal adenocarcinoma
PTM	–	Post-translational modification
RBP	–	RNA-binding protein
RNAi	–	RNA interference
RT	–	Room temperature
SEM	–	Standard error of the mean
SET	–	Su(var)3-9, Enhancer of Zeste, Trithorax
SpdS	–	Spermidine synthase
SUMO	–	Small ubiquitin-related modifier
SUnSET	–	Surface sensing of translation
tRNA	–	Transfer RNA
wt	–	wild-type

Introduction

Post-translational modifications

In 1990, an international group of researchers set out to uncover the blueprints of life: the sequence of the human genome and the location of the genes contained therein. The Human Genome Project was completed in 2003, and the consortium estimated that the human genome contains 20,000-25,000 protein-coding genes[1]. As the name implies, these genes are capable of being transcribed into RNA, processed into mRNA, and translated into protein. While the higher estimate of our genome is approximated at 25,000 protein-coding genes, the number of proteins in the human proteome is estimated at over one million. Due to various mechanisms, such as alternative splicing and alternative polyadenylation, one gene can give rise to multiple protein isoforms with potentially different biological functions[2,3]. In addition, the complexity of the human proteome is vastly increased by post-translational modification (PTM) of proteins. These modifications encompass the covalent attachment of a small chemical group, sugar moieties, or a protein domain to the amino acids that make up a protein. From ~130 putative and experimentally verified PTMs, phosphorylation, acetylation, ubiquitylation, succinylation, and methylation are the most commonly studied[4]. These PTMs can have major consequences to the function, localization, and interactions of the modified protein and impact various biological processes. For instance, changes in protein activity by phosphorylation via cyclin-dependent kinases is a critical mechanism for the progression of the cell cycle[5]. Furthermore, methylations on histone tails can be bound by various factors that can change the chromatin state, influencing transcription[6].

Protein methylation

Methylation involves the covalent addition of a methyl group (CH_3) to a substrate, which includes DNA[7], RNA[8], proteins[9,10], and various smaller molecules[11]. The methylation of amino acids in proteins is a prevalent type of PTM, and its discovery goes back to 1959, when a methylated lysine residue was found in flagellin from *Salmonella typhimurium*[12]. The occurrence of methylated lysines were reported in mammalian histones a few years later, along with the discovery that protein methylation is catalyzed by enzymes post-translationally as opposed to methylated residues being incorporated during protein synthesis[13,14]. The apparent conservation of protein methylation from bacteria to mammals along with the involvement of

enzymatic systems to introduce this PTM indicated a certain physiological importance. Today, it is known that specific protein methylations can serve functions in the regulation of chromatin state, fine-tuning of enzyme activity, mediation of subcellular localization, and modulation of protein interactions.

Although lysines were first discovered to be capable of being methylated, many other amino acids were found to contain this PTM as well. Lysines and arginines are found to be frequently methylated, but other residues, such as histidines and the N- and C-termini of proteins, can also be methylated[15–19]. The protein methylome of a single human cell line contains almost 5,000 methylation sites over 1,600 proteins between lysine, arginine, and histidine residues alone[20]. This extraordinary amount of protein methylation can even be found in simple eukaryotes such as yeast, which have been reported to contain around 300 unique methylation sites[21]. The vast expanse of protein methylation has caused many researchers to try to unravel the biological function of each methylation event, as well as the MTases responsible for adding, or 'writing', this PTM on various protein residues.

Methyltransferases

Methyltransferases (MTases) are specialized enzymes that are capable of catalyzing the transfer of a methyl group from a donor molecule to a substrate. MTases can target an immense range of substrates, and the majority of these enzymes utilize *S*-adenosylmethionine (AdoMet) as a methyl donor. In these cases, the MTase exposes the electron-rich target site of the substrate to the electron-deficient methyl group of AdoMet. This allows for a nucleophilic attack on the methyl group of AdoMet, resulting in the cleavage of the bond between the carbon atom of the methyl group and the sulfur atom of AdoMet[22]. The methyl group is then transferred to the substrate and leaves behind *S*-adenosylhomocysteine (AdoHcy).

When considering the vastness and variety of methylated substrates in human and yeast, it is not too surprising that MTases are abundant in both species, with 208 and 81 putative enzymes which encompass around 0.9% and 1.2% of gene-products, respectively[23,24]. Although the abundancy of MTases indicates an important role for methylation, what is even more striking is that 64% of protein MTases in yeast have a known human ortholog[21]. This conservation throughout evolution indicates a biological importance to the methylation of certain target sites. Their importance is further

emphasized by the finding that 30% of known and putative human MTases correlate with cancer and mental disorders[23]. In order to dissect the function a methylation mark may have in a biological system, it is critical to identify and characterize the responsible MTases. This identification typically involves knockout studies of the putative MTase in various models, which can also be applied for evaluating the biological effects the absence of a specific methylation mark may have. Bioinformatic analyses of conserved sequence motifs have been particularly useful in the identification of novel MTases, which are further classified according to their common structural arrangements into distinct superfamilies (**Figure 1**).

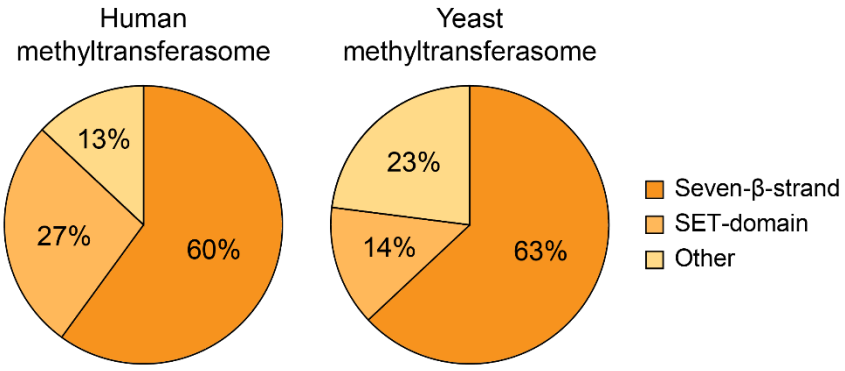

Figure 1: The human and yeast methyltransferasomes. The distribution of superfamilies in the methyltransferasome is depicted for known and putative MTases in human (left) and yeast (right). The figure is adapted from Petrossian and Clarke, 2011[23].

Seven-β-strand methyltransferases

The seven-β-strand (7BS) superfamily makes up around two thirds of the total methyltransferasome in both human and yeast, making it the most abundant class (**Figure 1**)[23]. The three-dimensional structure of 7BS MTases, as the name implies, consists of seven β-strands that are in most cases sandwiched between α-helices (**Figure 2**). The β-sheet of these MTases have a characteristic arrangement that is reminiscent of the Rossman-fold, with the first six β-strands running parallel to one another and the last β-strand having an anti-parallel orientation[25].

Furthermore, 7BS MTases can contain up to four homologous sequence motifs at distinct positions in their three-dimensional structure, which are denoted as motif I, motif post I, motif II, and motif III (**Figure 2**)[26,27]. Despite some family members lacking one or several of these hallmark motifs, they have been useful in the identification of

novel MTases and their modus operandi. For instance, residues in motif I and motif post I are capable of binding and positioning AdoMet, whereas motif II and III are involved in the binding of their susbtrate[26–28]. Interestingly, orthologous 7BS MTases from different organisms share a conserved stretch of residues following motif II, often referred to as motif post II, which is thought to be important for catalysis or substrate specificity[25,29].

The 7BS superfamily of MTases covers a wide range of substrates, such as DNA, RNA, and proteins[30]. Although the first identified 7BS lysine-specific MTase (KMT), DOT1L, was shown to target histone 3, none of the other 7BS KMTs have been found to methylate histones thus far[31]. Remarkably, 7 of the 16 characterized human 7BS KMTs methylate the translational apparatus. Most of these seven enzymes and all of their substrates are conserved in a wide range of eukaryotes[15].

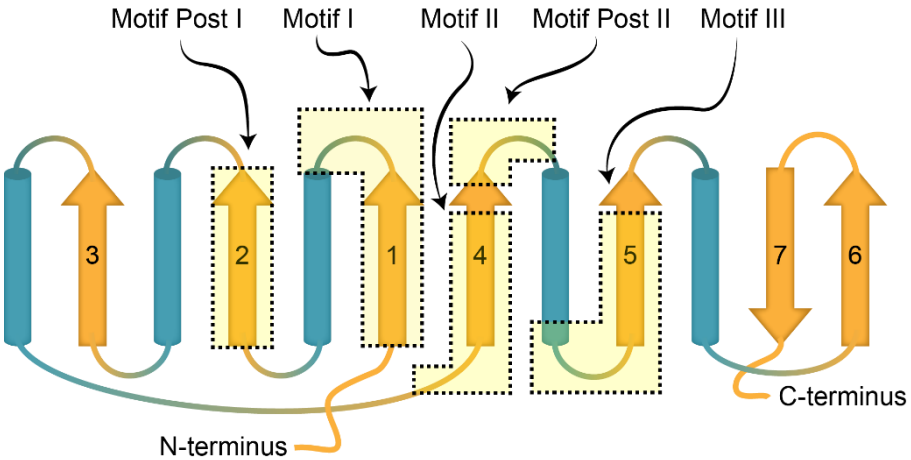

Figure 2: Schematic representation of the canonical 7BS fold. The seven β-strands are numbered in the N-to-C-terminal direction and colored orange, α-helices are colored turquoise. The areas highlighted in yellow depict the location of conserved motifs within the superfamily (motif I, motif post I, motif II, and motif III) or between orthologs of 7BS MTases (motif post II). The figure is adapted from Falnes, et al., 2016[25].

SET-domain methyltransferases

The SET-domain was initially discovered as a conserved domain in three *Drosophila melanogaster* enzymes, after which this domain was named: Su(Var)3-9, Enhancer of Zeste, and Trithorax[32]. This superfamily of MTases is widespread in eukaryotes, and is the second largest in both the human and yeast methyltransferasome, although proportionally larger in human (27%) than in yeast (14%) (**Figure 1**)[23]. This is partly due to a large presence of human SET-domain MTases that target histone proteins, suggesting that epigenetic regulation has a greater importance in humans. While 7BS MTases cover a wide range of substrates, the SET-domain superfamily consists almost exclusively of KMTs. Most of the SET-domain MTases target lysines on histone proteins, but some of these enzymes have been shown to target other proteins, as well as being capable of methylating histidine residues[33,34].

Lysine methylation

Lysine residues can receive up to three methyl groups on their ε-amine moiety. This leads to four possible species of lysine in the context of methylation: unmethylated, monomethylated, dimethylated, and trimethylated lysine (Kme0, Kme1, Kme2, Kme3 respectively) (**Figure 3A**). This methylation is catalyzed by KMTs, also referred to as methylation 'writers'. Gradual methylation of lysine residues increases its bulkiness and hydrophobicity and reduces its capability to form hydrogen bonds without affecting its overall positive charge[35].

Although the existence of methylated lysine residues was discovered in the late 1950s, it was not until 1986 before any functional data was linked to this PTM. At this time, a study showed that Kme3 at position 115 of calmodulin lowers its potential to stimulate the activity of the NAD kinase without affecting the activation of other calmodulin targets[36]. These findings showed for the first time that lysine methylation can modulate a specific function of a protein. The field entered its golden age at the turn of the millennium, when it was uncovered that lysine methylation is an important regulator of chromatin state and transcriptional activity. Methylation of lysine 4 on the tail of histone 3 (H3K4) was found to be highly conserved from unicellular eukaryotes to humans, and trimethylation in particular was found to only be present in actively transcribed genes[37,38]. In contrary to the association of methylated H3K4 with transcriptionally active genes, the methylation of lysine 9 on the tail of histone 3 (H3K9)

was linked to the establishment of transcriptionally silent heterochromatin[39,40]. Soon after, additional methylations were identified on various lysine residues on different histone tails[41]. It became evident that the position of the lysine residue on the histone tail and the degree of methylation (Kme0, Kme1, Kme2, or Kme3) could be linked to a transcriptional outcome. The influence of this PTM on chromatin accessibility was found to come not from the methylation mark itself, but rather from effector proteins that can bind, or 'read', methylated lysines[39,40]. Furthermore, different lysine-specific demethylases (KDMTs) were found to remove methyl groups from histone lysine residues, which uncovered the dynamic nature of histone methylation. Although these findings led to an explosive interest in protein methylation, it also swayed the field towards chromatin biology and overshadowed research of non-histone protein methylation.

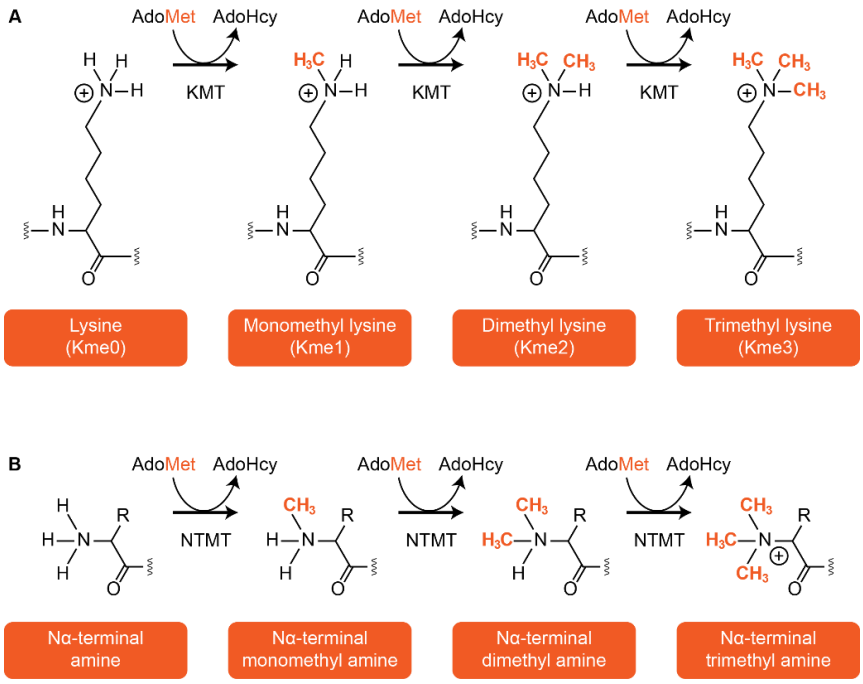

Figure 3: Schematic depicting the methylation of lysine residues and N-termini via MTases. A) Chemical structures of differentially methylated lysine residues on a polypeptide chain. Lysines can either lack a methyl group (Kme0), or be mono- (Kme1), di- (Kme2), or trimethylated (Kme3) by KMTs utilizing AdoMet as a methyl donor. **B)** Chemical structures of differentially methylated protein N-termini. The α-amino group can receive up to three methyl groups, a process that is catalyzed by NTMTs utilizing AdoMet as methyl donor.

N-terminal protein methylation

After the initiator methionine is cleaved off, the exposed α-amino group on the N-termini of proteins can be mono-, di-, or trimethylated by N-terminal MTases (NTMTs) (**Figure 3B**). In general, N-terminal monomethylation moderately reduces the reactivity of the N-terminal amino acid due to steric hindrance and increases the pK_a value with up to 0.5 units, whereas trimethylation would cause a permanent positive charge[42]. All N-terminal methylated forms have been found in biochemical assays but trimethylation is most commonly observed *in vivo*. Although N-terminal methylation was first documented over 40 years ago in bacterial ribosomal proteins, it has remained largely unexplored relative to lysine methylation[43]. A recent estimate found that approximately 7-8% of the yeast and human proteome undergoes N-terminal methylation[44]. This PTM is thought to be irreversible due to the absence of identified N-terminal demethylases, suggesting that N-terminal methylation could potentially be a permanent modification. Thus far, only three NTMTs have been identified: NTMT1, NTMT2, and methyltransferase-like protein 13 (METTL13). NTMT1 and NTMT2 are structurally highly similar and are known to target a broad range of protein substrates[45,46]. This is in contrast to METTL13, which only targets the eukaryotic translation elongation factor 1 alpha (eEF1A)[47]. Curiously, the N-terminal methylation of eEF1A is conserved from human to yeast but the responsible enzymes are distantly related[47,48]. The enzymes seem to have arisen twice throughout the course of evolution, suggesting a functional benefit of this PTM on eEF1A.

Elongation factor 1 alpha

The translation of mRNA into protein involves three main steps: initiation, elongation, and termination. Protein translation is catalyzed by several translation factors during these distinct steps. During the elongation phase of translation, eEF1A in its guanosine-5'-triphosphate (GTP) -bound form can bind and deliver an aminoacyl-tRNA (aa-tRNA) to the A-site of the translating ribosome. When a correct codon-anticodon pairing is formed, the ribosome undergoes a conformational change. This leads to GTP hydrolysis of eEF1A and its release from the translating machinery in its guanosine-5'-diphosphate (GDP) -bound form. The eEF1A-GDP complex can then be reactivated via the nucleotide exchange factor eukaryotic elongation factor 1 beta (eEF1B), at which point eEF1A can continue the cycle of binding a new aa-tRNA and deliver it a vacant A-site on the ribosome (**Figure 4**).

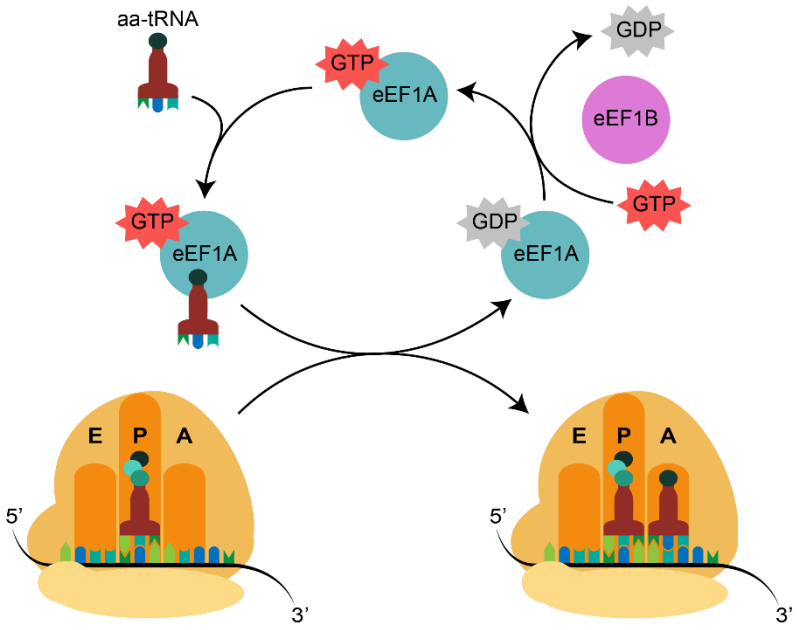

Figure 4: The function of eEF1A during translation elongation. eEF1A in complex with GTP delivers aa-tRNAs to the A-site of translating ribosomes. GTP is hydrolyzed upon correct codon-anticodon binding, causing eEF1A to be released in a complex with GDP. The nucleotide exchange factor eEF1B facilitates the exchange of GDP for GTP on eEF1A, allowing the new cycle to begin.

Due to its function in such a vital process, it is not surprising that eEF1A is highly conserved and is one of the most abundant cellular proteins (~3%). Many organisms contain more than one gene encoding eEF1A, in mammals it is expressed in the form of two highly similar paralogs: eEF1A1 and eEF1A2 (92% identical at the amino acid level). Both paralogs consist of three structural domains that function in GTP binding (domain I), aa-tRNA binding (domain II), interaction with eEF1B for GDP to GTP exchange (domain I and II), and actin binding (domain III). Although the paralogs were shown to have similar translational activity in an *in vitro* system, their relative binding affinity for GDP and GTP slightly differs[49]. The most striking difference between the eEF1A paralogs are their expression patterns, eEF1A1 is ubiquitously expressed throughout development but is replaced by eEF1A2 in brain, heart and muscle tissues[50].

The methylation landscape of eEF1A and its writers

eEF1A contains various PTMs, including many methylations. Specifically, the methylation landscape of human eEF1A consists of five methylated lysine residues (K36, K55, K79, K165, and K318) and a trimethylated N-terminus (G2) (**Figure 5**)[51]. Some of these methylation sites, along with the enzymes that catalyze them, have been shown to be highly conserved in eukaryotes. For instance, N6AMT2 and METTL10 were identified as the KMTs responsible for trimethylating eEF1A on K79 and K318, respectively, due to their sequence similarities to two characterized yeast KMTs with the same function[48,52]. Other methylation marks on human eEF1A are not conserved in yeast, such as dimethylation of K55 (K55me2) or trimethylation of K36 and K165. Thus, the responsible KMTs were identified via different strategies. Based on the sequence and structure of ECE2 and METTL21B, the proteins were found to contain a putative 7BS MTase domain. Via *in vitro* MTase assays on human cell extracts, mass spectrometry (MS) substrate identification, and CRISPR-Cas9 (clustered regularly interspaced palindromic repeats and CRISPR-associated protein 9) knockout validation, ECE2 and METTL21B were found to trimethylate K36 and K165 (respectively) on human eEF1A[53,54]. Using a different approach, K55me2 on human eEF1A was found to be dependent on METTL13 when comparing wild-type and knockout HAP-1 cells in an MS-screen[47]. This was confirmed by another study, which knocked out 107 known or putative KMTs in U20S cells and found that only the

knockout of METTL13 abolished K55me2 on eEF1A[55]. Interestingly, G2 trimethylation (G2me3) of eEF1A is conserved between yeast and human, and while the MTase responsible for this mark was identified in yeast, it lacks a clear human ortholog[48]. *In vitro* and *in vivo* work showed that another domain of METTL13, which shares no homology with the corresponding yeast MTase, is in fact responsible for the G2me3 mark on human eEF1A[47].

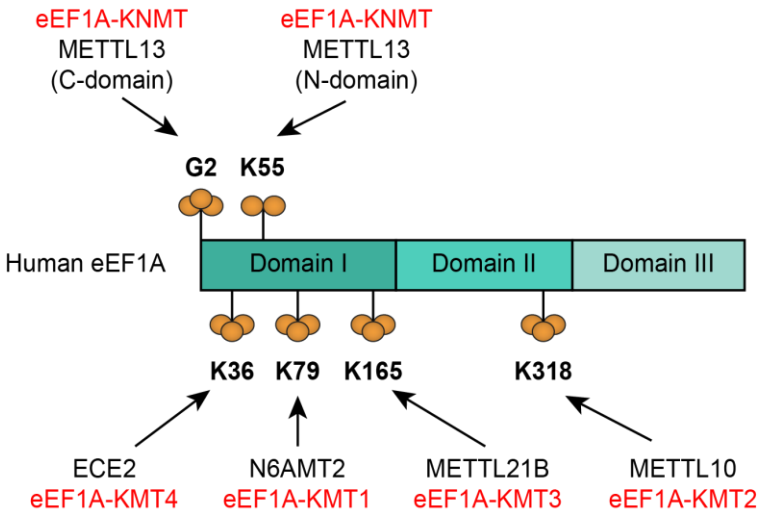

Figure 5: The methylation landscape of human eEF1A and the responsible MTases. The methylated residues on human eEF1A are shown in bold, the number of orange spheres indicates mono-, di-, or trimethylation of the associated residue. Arrows indicate the responsible MTase for each methylation mark. A newer nomenclature for each MTase is shown in red. Image is adapted from Engelfriet, et al., 2023[56].

METTL13 – a dual methyltransferase

In contrast to the other MTases targeting human eEF1A, METTL13 is responsible for catalyzing the methylation of two residues (K55 and G2) as opposed to a singular residue[47]. This dual function is achieved through two distinct MTase domains: one being N-terminal and the other C-terminal. The separate domains will be referred to as MT13-N and MT13-C henceforth. Based on their sequences, both MTase domains of METTL13 belong to the 7BS superfamily but are not very closely related. The closest paralog for MT13-C was found to be spermidine synthase (SpdS), an enzyme with no MTase activity. Nonetheless, MT13-C was found to distinctly trimethylate G2 of eEF1A, and the structure of MT13-C is reminiscent of the classic 7BS fold (**Figure 6A**)[47]. In contrast to MT13-C, MT13-N has three close paralogs, which are all

established KMTs. Specifically, MT13-N belongs to a subfamily of 7BS MTases which share a conserved [D/E]-K-G-T-X-D sequence in motif post II between the family members and their orthologs in different organisms[54]. The other family members are known to either methylate lysine residues on eEF1A (ECE2 and METTL10), or citrate synthase (METTL12)[57]. The theoretical 3D structure of MT13-N indicates a possible 7BS fold, and the MTase has been experimentally verified by two independent studies to dimethylate K55 on eEF1A (**Figure 6B**)[47,55]. Bioinformatic analysis indicates that METTL13 and motifs from both MTase domains are conserved in multicellular eukaryotes, with putative orthologs present in common model organisms such as mouse, nematode and fruit fly (**Figure 6C**)[54]. While METTL13 has been found to target two residues of eEF1A for methylation, there is no indication of other substrates for either MTase domain[47,55]. The specificity for G2 and K55 on eEF1A, along with the conservation of both the enzyme and the substrate, give an indication of a certain importance to these methylation marks.

Regulation of METTL13

Both the expression and enzymatic activity of METTL13 have been found to be subject to regulation through various mechanisms. For instance, METTL13 transcription can be upregulated by HN1L through the transcription factor Ap-2γ[58]. Furthermore, the microRNA miR-16 can bind the 3'UTR of METTL13 mRNA and negatively regulate its translation[59,60]. On the protein level, METTL11A has been reported to bind METTL13 and regulate its methylation activity by promoting K55 methylation and inhibiting N-terminal methylation on eEF1A[61]. These findings indicate a necessity for tight control over the activity of METTL13.

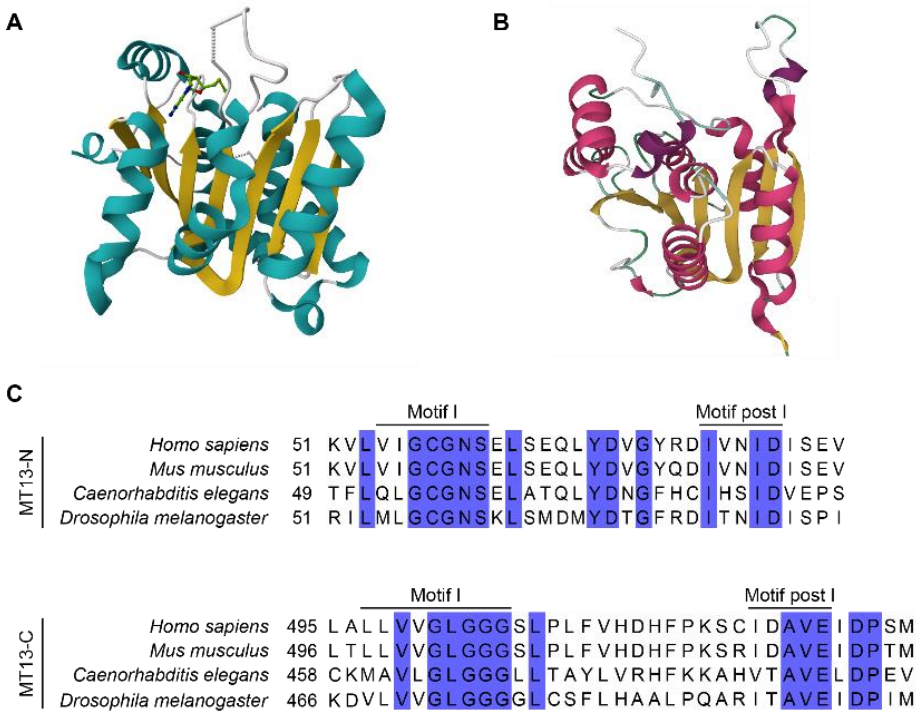

Figure 6: MT13-N and MT13-C belong to the 7BS superfamily of MTases. A) The solved structure of MT13-C (PDB ID: 5WCJ) contains the canonical 7BS fold, with the β-strands shown in yellow and alpha helices in turquoise. **B)** Theoretical 3D structure encompassing human MT13-N indicates that the MTase may contain a 7BS fold. The structure was generated by AlphaFold, amino acids 1-215 of METTL13 (UniProt ID: Q8N6R0) are depicted, with β-strands shown in orange and alpha helices in magenta. **C)** Multiple sequence alignment of MT13-N and MT13-C from human METTL13 with putative orthologs in mouse (*Mus musculus*), nematode (*Caenorhabditis elegans*), and fruit fly (*Drosophila melanogaster*) reveals conservation of residues in motif I and motif post I in both domains.

Multiple PTMs have been reported on human METTL13 (**Figure 7**). Various types of PTMs can alter the function, subcellular location, or stability of a protein. For instance, phosphorylation can function as a molecular switch to control the activity, but also the stability of its substrate[62]. The covalent addition of polypeptides such as ubiquitin and small-ubiquitin related modifier (SUMO) are known to target substrates for proteasomal degradation[63,64]. In contrast, the addition of ubiquitin and SUMO monomers have non-proteolytic functions in processes such as transcriptional regulation and DNA repair by modifying protein activity and localization[65,66]. All of these three types of PTMs, phosphorylation, ubiquitylation, and SUMOylation, have been reported to occur on human METTL13. The residues K88, T129, K134, S506,

K600, S603, and T606, belonging to the MTase domains, have also been found to be phosphorylated and ubiquitylated. The significance of these PTMs and whether they may regulate METTL13 is not yet understood.

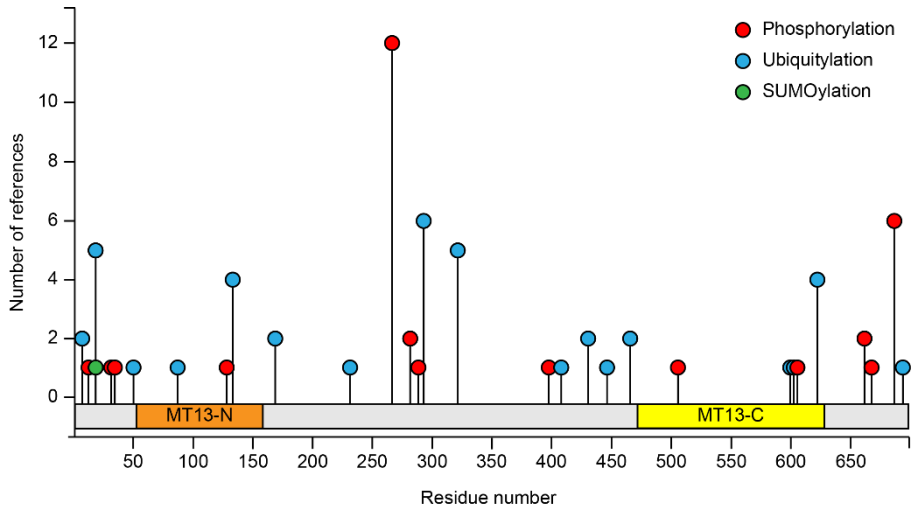

Figure 7: Human METTL13 displays a rich PTM landscape. The position of residues that have been reported to be phosphorylated, ubiquitylated or SUMOylated on human METTL13 are indicated by red, blue, and green spheres, respectively. The data was obtained from PhosphoSitePlus (accessed on 4th of September 2023)[67].

METTL13 in health and disease

In 2011, METTL13 was first described to be overexpressed in a plethora of human cancers, leading to it being named Faint Expression in normal tissues, Aberrant overexpression in Tumors (FEAT) at the time[68]. Since then, more studies have shown that METTL13 expression and eEF1A^{K55me2} is upregulated in numerous human cancers and correlates with poor patient prognosis[55,69,70]. Various human cancer cell lines decline in proliferation and global protein synthesis upon ablation of METTL13, further strengthening the link to cancer[55,69]. Furthermore, abolishment of METTL13 function in xenograft mouse models and depletion of pancreatic METTL13 in pancreatic ductal adenocarcinoma (PDAC) mice has also been shown to suppress tumor growth[55,69].

Interestingly, regulators of METTL13 have been linked to cancer as well. The expression of miR-16 is low in lung, breast, and hepatocellular cancer tissues compared to normal adjacent tissues[59]. Hepatocellular cancer patients with low expression of miR-16 also tend to have a poorer prognosis[60]. Since miR-16 negatively regulates METTL13 post-transcriptionally, these studies indicate that low levels of miR-16 could be responsible for the overexpression of METTL13 seen in cancers. While both mice models and human cell lines have been useful in uncovering the role of METTL13 in tumorigenesis, they each have their individual limitations for studying this enzyme in both health and disease. For instance, human cancer cell lines do not recapitulate the inherent complexity of an *in vivo* system and certain physiological aspects of life cannot be assessed *in vitro*. While mouse models are advantageous in these regards, experiments such as lifespan assays are more time consuming (~2.5-3 years) compared to other model organisms.

Caenorhabditis elegans as a model organism

The free-living nematode *Caenorhabditis elegans* (*C. elegans*) was introduced as a model in 1963 by Sydney Brenner as a model system to genetically dissect neurobiology and development[71]. Today, this nematode is studied in thousands of laboratories around the world in various biological contexts, due to its many advantages. Its small size (1 mm) and optical transparency allow for non-invasive microscopic assessment of the animals on the cellular level[72]. The power of this model organism is further strengthened by the ease of manipulating gene expression and accessibility to a well-developed genetic toolkit. For instance, two RNA interference (RNAi) libraries encompassing 11,804 and 16,757 RNAi clones are available for knocking down most of the predicted genes in *C. elegans* (78% and 86% respectively)[73,74]. Furthermore, mutant strains carrying a specific deletion resulting in gene knock-out are available through the *C. elegans* Gene Knockout Consortium and the National Bioresource Project (NBRP) in Japan. At the turn of the century, *C. elegans* became the first multicellular eukaryote to have its genome sequenced[75]. Together with the unveiling of the human genome, this gave a first insight into the extensive homology the two genomes shared. *C. elegans* orthologs have been identified for an estimated 60-80% of human genes, encompassing many biological and biochemical pathways that are conserved from nematode to human[76–78]. It is

thanks to this simple model organism that research groups were able to make breakthrough discoveries in highly conserved mechanisms such as apoptosis and RNAi[79,80]. Furthermore, 42% of human genes that are associated with disease have an ortholog in *C. elegans*[81].

Most *C. elegans* animals are self-fertilizing hermaphrodites and can give rise to a large number of homozygous progeny, meaning that a homozygous mutation can be preserved throughout generations[72]. Lethal or sterile mutations on essential genes can be maintained in heterozygotes via genetic balancers such as chromosomal rearrangements, preventing the loss of the mutation through segregation[82]. Males can also occur in the population through non-disjunction of the X-chromosome during meiosis. Although they are capable of generating heterozygous offspring through mating with hermaphrodites, which can cause the loss of a mutation, they rarely arise in normal laboratory conditions (~0.1%)[72]. Another advantage is that the life cycle of *C. elegans* is relatively short under favorable conditions. Individuals hatch from eggs and develop through four larval stages (L1, L2, L3, and L4) before reaching fertile adulthood in less than 3 days, with their total lifespan being approximately 3 weeks (**Figure 8**)[72]. This short lifespan has made *C. elegans* a particularly popular model organism in aging-related research.

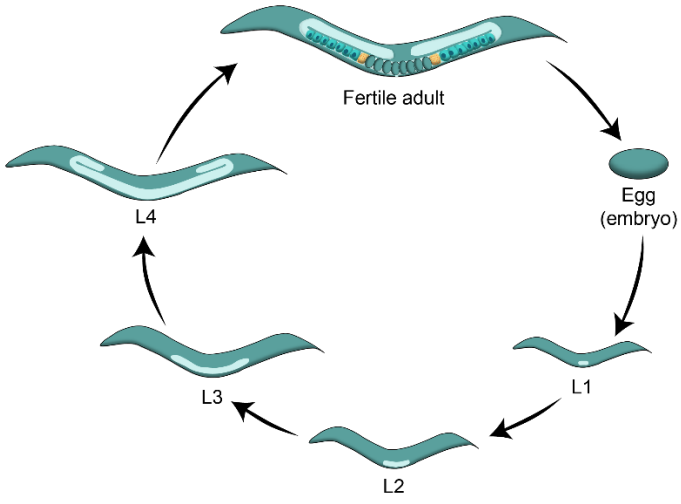

Figure 8: The *C. elegans* life cycle. *C. elegans* embryos develop both *in utero* and *ex utero* in an egg. After egg-hatching, animals develop through subsequent larval stages (L1, L2, L3, and L4) before reaching adulthood.

C. elegans as a cancer model

Cancer is a complex disease that originates from the oncogenic transformation of one or a few cells with the ability to spread to other parts of the body. Due to the complexity with which tumors can acquire different kinds of malignant properties, researchers have turned to model organisms that can offer a simplified understanding of tumorigenesis. For instance, unicellular yeast species have been used to unravel how the cell cycle is controlled, which is orchestrated by proteins that are highly conserved and are now often found to be dysregulated in human tumors[83]. Additionally, human cancer cell lines have been used to identify oncogenes and tumor suppressor genes, which has aided in the characterization of dysregulated pathways in cancer. The identification of pathways that are dysregulated and promote tumorous growth has been beneficial in understanding cancer etiology and drug design. However, these models lack distinct tissues and organ systems in which these tumors develop. *C. elegans* has emerged as a model for genetic dissection the molecular foundation of tumorigenesis in humans. Many genes that are implicated in cancer development are conserved in *C. elegans*[81]. Moreover, the function of these genes are easier to dissect in the nematode as the gene families consisting of fewer members, thus reducing genetic redundancy[81,84]. One prominent hallmark of cancer is sustained proliferative signaling to drive neoplastic growth[85]. Genetic screens in *C. elegans* have aided in characterizing novel components of proliferative signaling pathways and their cross-talk during human pathology[86]. Although genetic manipulation of *C. elegans* can result in cell cycle defects in somatic cells, they never give rise to a tumor-like phenotype, as the animal almost completely exists out of post-mitotic cells. In contrast, dysregulation within the germline can give rise to hyperproliferation of germ cells and bona fide tumors. One such example is the dysregulation of the highly conserved Notch signaling pathway, which regulates stem cell renewal. In this pathway, the Notch receptor binds signaling ligands, which leads to the activation of a transcriptional response that specifies the stem cell fate[87,88]. Dysregulated Notch signaling has been implicated in a plethora of human cancers, making it a potential therapeutic target. In *C. elegans*, Notch hyperactivation leads to mitotic proliferation of early germ cells, resulting in a tumorous phenotype[89]. The severity of this germline tumor can be visualized under various genetic conditions by whole animal microscopy. Such studies can reveal suppressors and enhancers of Notch signaling and a further understanding

of this pathway that may aid in identifying potential therapeutic targets in human cancers[90,91].

Intriguingly, the pathways involved in germ cell proliferation and development, including Notch signaling, are post-transcriptionally regulated in the *C. elegans* germline. This regulation is largely mediated by RNA-binding proteins (RBPs), which bind specific mRNA targets through sequences or structures in the untranslated regions (UTRs)[92]. One example is GLD-1, an RBP which directly binds and represses the translation initiation of various transcripts, including those encoding cell cycle regulators and the Notch receptor GLP-1[91,93–95]. Loss of GLD-1 function results in the inappropriate translation of its targets, causing their ectopic expression and the formation of germline tumors[93,94]. Perturbations in translational control are also apparent in human cancers. Overexpression or dysregulation of translation initiation factors can cause an increase in protein synthesis, which can contribute to oncogenic transformation or sustained tumorous growth[96,97]. Since translation initiation is the first step of protein synthesis, many studies have focused on how the factors involved in this process are aberrantly regulated during tumorigenesis. Although translation elongation has been much less studied, the dysregulation factors involved in this process have been acknowledged to be similarly important for tumorous growth[96,98].

Aims of this thesis

The general aim of this thesis is to characterize the biochemistry and function of METTL13 in *C. elegans* in the contexts of both health and disease. This main goal is further divided into smaller aims:

- Assess if the methylation marks on eEF1A on residues G2 and K55 are conserved in *C. elegans*.

- Evaluate if the putative *C. elegans* ortholog of METTL13 displays dual-MTase activity on eEF1A.

- Establish if *C. elegans* can be used as a cancer model in the context of METTL13.

- Characterize the effects of lack of METTL13 in a whole animal during normal physiological conditions.

- Establish if METTL13 plays a role during various stress conditions.

Methodology

General maintenance of *C. elegans*

Animals were cultivated on 6 cm^2 nematode growth medium (NGM) agar plates (0.25% (w/v) tryptone, 0.3% (w/v) NaCl, 1.5% (w/v) agar, 1 mM $CaCl_2$, 1 mM $MgSO_4$, 25 mM KPO_4 pH 6.0, and 5 µg/mL cholesterol) with *Escherichia coli* (*E. coli*) OP50 as the food-source as previously described, unless stated otherwise[71]. For the purpose of general maintenance, all strains were kept at 20°C.

Synchronization by bleaching

To obtain synchronized animals, gravid adults were harvested from NGM plates with 1x M9 buffer (42 mM Na_2HPO_4, 22 mM KH_2PO_4, 86 mM NaCl, 1 mM $MgSO_4$) in a 15 ml conical tube and pelleted by centrifugation for 1 minute at 1,500 rpm. The supernatant was aspirated, and the eggs were extracted from gravid adults by 5-7 minutes of treatment with 7 ml bleaching solution [30% (v/v) sodium hypochlorite (5% chlorine) reagent (ThermoFisher Scientific; 419550010), 750 mM KOH]. Once the eggs were extracted and the debris was dissolved, the bleaching solution was removed by centrifugation at 1,500 rpm for 1 minute followed by aspiration. To remove any residual bleaching solution, the eggs were washed thrice in 1x M9. Each wash consisted of the addition of 10 ml 1x M9, followed by centrifugation at 1,500 rpm for 1 minute and aspiration of the supernatant. Finally, the eggs were resuspended in 10 ml 1x M9 and left to hatch overnight at room temperature (RT) on a bench-top rocker into arrested L1 larvae.

Freezing and thawing

C. elegans strains can be stored for long periods of time at -80°C or in liquid nitrogen. Animals were grown until the plate consisted mostly of L1-L2 stage larvae that were starved for one day. Harvesting was accomplished by washing the animals off the plates with 1x M9 buffer and collecting in a 15 ml conical tube. The animals were pelleted by centrifugation at 1,500 rpm for 1 minute and resuspended in 200 µl freezing solution [3% (w/v) trehalose dihydrate, 3.5% (v/v) DMSO in 1x M9 buffer] per harvested plate. For each frozen stock, 150 µl was aliquoted per 2 ml cryogenic tube. The tubes were placed on ice and transferred to -80°C. For each newly frozen down strain, seven tubes were prepared, of which one would always be thawed after 24 hours of freezing to assess the viability of the frozen stocks. When thawing a frozen strain, a tube was collected from -80°C and brought to room temperature until the ice had melted. The animals were gently transferred by pipetting 25-100 µl of the stock onto an NGM plate containing *E. coli* OP50. Animals were examined for recovery after 2 hours by stereoscopic microscopy.

C. elegans crossing

Crossing was used for two purposes: I) the generation of a strain containing the combined genotype of the parental strains, and II) outcrossing of a mutant strain to wild-type. The first purpose was used, for instance, to generate a double-mutant strain. Outcrossing was done to eliminate unwanted background mutations in a mutant strain, which could have occurred as a by-product of genome editing methods such as CRISPR-Cas9. In order to cross two animals of a different genotype, males are needed, which naturally appear at low frequencies (0.2%)[99]. In order to increase the incidence of males in the progeny of a strain, L4 larvae were heat-shocked for 6 hours at 30°C and then shifted to 25°C to lay offspring. Once the progeny reaches adulthood, 10-15 of the males were transferred to a crossing plate (3 cm^2 NGM plate containing *E. coli* OP50). Four hermaphroditic L4 larvae of the second strain of interest were moved onto the same plate and kept at 25°C for 24 hours. Gravid hermaphrodites were singled onto separate crossing plates and kept at 25°C until it was possible to observe the sex of the F1 progeny by stereoscopic microscopy. Plates that contained 50% males in the F1, indicating mating, were kept. Four hermaphroditic L4 larvae from

this generation were further singled onto separate crossing plates to lay the F2 progeny at 25°C. From the F2, 20-25 hermaphroditic L4 larvae were singled onto separate crossing plates to lay eggs at 25°C. Once a minimum of around 50 eggs were laid, the F2s were genotyped by PCR, sequencing or a combination of PCR and confocal microscopy.

Extraction of genomic DNA for genotyping by PCR

After crossing, F2 adults were separately transferred to 0.2 ml tubes containing 10 µl lysis buffer [52 mM KCl, 10 mM Tris pH 8.3, 2.5 mM $MgCl_2$, 0.45% NP40, 0.45% Tween 20, 0.05% gelatin in ddH_2O] and lysed (60°C for 1 hour, 95°C for 15 minutes, 8°C indefinitely). Genotyping PCR reactions were set-up using the Q5 High-Fidelity DNA polymerase (New England BioLabs) according to the protocol of the manufacturer, specific genotyping primers (see **Table 1**), and 1 µl of genomic DNA. PCR products were analyzed by agarose gel electrophoresis and verified by Sanger sequencing.

Table 1: Primers used for genotyping of strains after crossing.

Primer	Sequence (5' → 3')
metl-13(tm6870) fwd	ATGGCCGATGAAGCACATAC
metl-13(tm6870) rev	CGGCGAATGTGTCAATCTT
eef-1A.1(syb2837) fwd	CAACGAGAGGGGGAGAGATT
eef-1A.1(syb2837) rev	TTGGGACGAATGGAACAGC
eef-1A.2(syb2785) fwd	GCACACCTATCACGTTCGTT
eef-1A.2(syb2785) rev	GGAGTCATTAGTGATGATCA

C. elegans strains

Information on the *C. elegans* strains used in this research is listed in **Table 2**. The *eef-1A.1(syb2837)* and *eef-1A.2(syb2785)* strains were designed by the author and generated separately by SunyBiotech using CRIPSR-Cas9 technology, resulting in animals endogenously expressing K55R mutated EEF-1A.1 and EEF-1A.2 respectively. These strains were crossed to obtain the *eef-1A.1(syb2837); eef-1A.2(syb2785)* double mutant. The *metl-13(tm6870)* strain was outcrossed three times with wild-type males, and the *eef-1A.1(syb2837); eef-1A.2(syb2785)* strain was similarly outcrossed nine times to reduce background mutations.

Table 2: *C. elegans* strains used in this research.

Strain genotype	Source	Identifier
Wild type	CGC*	N2
metl-13(tm6870) (IV)	NBRP	RAF2267
eef-1A.1(syb2837) (III); eef-1A.2(syb2785) (X)	Ciosk lab	RAF2260
pro-1(na48)/mIn1[dpy-10(e128) mIs14] (II)	CGC*	GC565
metl-13(tm6870) (IV); lin-41(rrr3) (I); xeSi197[Plin-41::flag::gfp::lin-41::lin-41 3'UTR; unc-119(+)] (II)	Ciosk lab	RAF2265
eef-1A.1(syb2837) (III); eef-1A.2(syb2785) (X); lin-41(rrr3) (I); xeSi197[Plin-41::flag::gfp::lin-41::lin-41 3'UTR; unc-119(+)] (II)	Ciosk lab	RAF2266

* *Caenorhabditis* Genetics Center

RNA extraction

Animals were collected from 6 cm^2 NGM agar plates with 1x M9 in a 1.5 ml Eppendorf tube. The mix of embryos, larvae, and adults was pelleted by centrifugation at 1,500 x g for 1 minute, after which the supernatant was removed. For each 100 µl pellet of animals, 250 µl Trizol was added before snap-freezing in liquid nitrogen. Animals were lysed by 10 freeze-thaw cycles with liquid nitrogen followed by incubation at 37°C. Nucleic acids were separated by chloroform extraction, during which 50 µl chloroform was added and the sample was mixed by inverting the tube multiple times before centrifugation at 12,000 x g for 10 minutes. The aqueous phase was transferred to a clean 1.5 ml Eppendorf tube and mixed by vortexing with 1 volume of isopropanol before centrifugation at 16,100 x g for 20 minutes at 4°C. Finally, the pellet was washed with 80% ethanol and air-dried before being resuspended in 25 µl nuclease-free water. The quality of the RNA was assessed by a NanoDrop Spectrophotometer.

cDNA synthesis

The QuantiTect Reverse Transcription kit (Qiagen) was used in line with the instructions from the manufacturer for the elimination of genomic DNA and reverse transcription of 1 µg of RNA. The resulting cDNA was diluted 1:5 for downstream RT-qPCR.

RT-qPCR

Gene expression analysis of *metl-13* and *act-1* was achieved via RT-qPCR using the HOT FIREPol EvaGreen qPCR Mix (Solis BioDyne) and the LightCycler 96 System (Roche). The components of the RT-qPCR mix are detailed in **Table 3**, the used cycler program is detailed in **Table 4**. The gene-specific primers pairs contained at least one primer spanning an exon-exon region and are listed in **Table 5**. The log fold change of *metl-13* relative to *act-1* expression was calculated via the delta-delta Ct method.

Table 3: Reaction components used for RT-qPCR.

Component	Volume (µl)
HOT FIREPol EvaGreen qPCR Mix	2 µl
Forward + reverse primer mix (10 µM)	0.25 µl
cDNA (1:5 diluted)	2.5 µl
Nuclease-free water	5.25 µl

Table 4: Thermocycling conditions used for RT-qPCR.

Step	Temperature	Time	Cycles
Pre-incubation	95°C	12 minutes	1
Denaturation	95°C	15 seconds	40
Annealing	60°C	20 seconds	
Extension	72°C	20 seconds	
Melting	95°C	10 seconds	1
	65°C	60 seconds	

Table 5: Primers used for gene expression analysis via RT-qPCR.

Primer	Sequence (5' → 3')
act-1 fwd	TTGCCCCATCAACCATGAAGA
act-1 rev	TGTGCAAGTTGACGAAGTTGTG
metl-13 fwd	CGGAATTAGCGACCCAACTCT
metl-13 rev	TCGGCCATGGATAGATTAGCA

Protein sample preparation

Animals were collected from 6 cm^2 NGM agar plates with 1x M9 in a 1.5 ml Eppendorf tube. The mix of embryos, larvae, and adults was pelleted by centrifugation at 1,500 x g for 1 minute, after which the supernatant was removed, and the pellet was snap-frozen in liquid nitrogen. Pellets were ground thrice into a fine powder with a pre-cooled mortar and pestle, liquid nitrogen was added between grindings. The powder was transferred to a 15 ml conical tube with a pre-cooled spoon, dissolved in 2x volume of lysis buffer [50 mM HEPES (pH 7.4), 150 mM KCl, 5 mM $MgCl_2$, 0.1% Triton X-100, 5% glycerol (w/vol), 1 mM PMSF, 7 mg/ml Complete™ (EDTA-free) protease inhibitor cocktail (Roche)], and lysed for 30 minutes at 4°C on a rotator. The lysate was cleared by centrifugation at 16,100 rcf for 20 minutes at 4°C and the cleared lysate was transferred to a clean 1.5 ml microcentrifuge tube. The protein concentration was estimated by Bradford Assay using a BSA protein standard curve. SDS-PAGE samples were prepared using 25 µg of total protein, 4x NuPAGE™ LDS Sample Buffer (Invitrogen, NP0007) and 10x NuPAGE Sample Reducing Agent (Invitrogen, NP0004). Finally, samples were incubated at 70°C for 10 minutes and stored at -20°C or directly used for SDS-PAGE.

Western blot

Proteins were separated by size using SDS-PAGE. For this purpose, samples were loaded on a 10-well NuPAGE™ 4 to 12%, Bis-Tris, 1.0 mm protein gel (Invitrogen) along with 5 µl of the Chameleon Dual Ladder (LI-COR). SDS-PAGE was run in 1x MES buffer in the Mini Blot Module (Invitrogen) at 200 V, 3000 mA, and 350 W for 30 minutes. Proteins were transferred from the gel onto a PVDF membrane (Millipore, IPFL00010) in the Mini Blot Module (Invitrogen) at 20 V, 3000 mA, and 350 W for 1 hour in 1x transfer buffer (Invitrogen) containing 10% methanol. Transferred proteins were visualized on the membrane by staining for 30 seconds with Ponceau S (Sigma), after which the staining was removed by rinsing in dH_2O. The membrane was dipped in methanol and air-dried before being transferred to a 50 ml conical tube. Methanol was washed over the membrane followed by three washes with ddH_2O. The membrane was blocked with 1:1 Blocking buffer (LI-COR) and 1x TBS for 1 hour at RT on a roller. Primary antibodies of interest (listed in **Table 6**) were diluted in 1:1

Blocking buffer and 1x TBS before being incubated with the membrane at 4°C overnight on a roller. Unbound antibodies were washed off the membrane thrice with 1x TBS-T for 5 minutes and secondary antibodies (listed in **Table 6**) diluted in 1:1 Blocking buffer and 1x TBS were incubated with the membrane at RT for 1 hour on a roller. Unbound secondary antibodies were removed by washing the membrane twice in 1x TBS-T and once in 1x TBS for 5 minutes. Bound antibodies were detected on the membrane with the Odyssey CLx Near-Infrared Fluorescence Imaging System (LI-COR).

Table 6: Antibodies used in this research.

Antibody	Dilution	Source
Mouse anti-eEF1A	1:1,000	Merck, 05–235
Mouse anti-puromycin	1:10,000	Merck, MABE343
Rabbit anti-actin	1:5,000	Abcam, ab8227
IRDye 680RD-conjugated goat anti-mouse	1:20,000	LI-COR Biosciences, 926–68070
IRDye 800CW-conjugated goat anti-rabbit	1:20,000	LI-COR Biosciences, 926–32211

Cloning of METL-13 domains

In order to assess the activity of the two METL-13 protein domains, the ORFs encoding the N-terminal (MT13-N: amino acids 1-417) and C-terminal domain (MT13-C: amino acids 213-656) were cloned separately. The two respective ORFs were PCR-amplified from *C. elegans* cDNA using the primers listed in **Table 7**. The MT13-N or MT13-C ORF was cloned, by using the In-Fusion HD Cloning Plus kit (Takara), into the pET28a plasmid (Novagen) between the NdeI and NotI sites, yielding encoded proteins carrying an N-terminal 6xHis-tag. The cloned constructs were verified by Sanger sequencing.

Table 7: Primers used for cloning of the *C. elegans* METL-13 domains.

Primer	Sequence (5' → 3')
MT13-N-NdeI-F	CGCGGCAGCCATATGTCCGCTCCAAATGAGC
MT13-N-NotI-R	CTCGAGTGCGGCCGCTTATTTCAGATAAGCTTCAGATTGTAC
MT13-C-NdeI-F	CGCGGCAGCCATATGCCTCTAGAAGTTCTTCGCTCC
MT13-C-NotI-R	CTCGAGTGCGGCCGCTTAATAATCAACCATACGAATGTTTGAG

Expression and purification of recombinant proteins

The MT13-N and MT13-C constructs were transformed into the *E. coli* BL21-CodonPlus(DE3)-RIPL strain (Agilent) according to the instructions of the manufacturer. Expression of recombinant MT13-N and MT13-C was induced overnight with 100 µM IPTG at 18°C. Lysis of bacteria and purification of 6xHis-tagged MT13-N and MT13-C was performed at 4°C. The bacteria were lysed in lysis buffer [50 mM Tris-HCl pH 7.4, 500 mM NaCl, 1% Triton X-100, 5% glycerol, 25 mM imidazole, 7 mg/ml Complete™ (EDTA-free) protease inhibitor cocktail (Roche), 10 U/ml Benzonase nuclease (Sigma-Aldrich)] and the lysates were cleared by centrifugation at 45,000 rcf for 30 minutes. Purification of 6xHis-tagged MT13-N and

MT13-C was performed using Ni-NTA-agarose (Qiagen) according to the instructions of the manufacturer. The protein concentration was estimated by use of the Pierce BCA Protein Assay Kit (Thermo Fisher Scientific). Purified proteins were stored in storage buffer [50 mM Tris–HCl pH 7.4, 100 mM NaCl, 10% glycerol] at -20°C in single-use aliquots.

In vitro methyltransferase assay

To assess the methylation activity of the METL-13 domains *in vitro*, a methyltransferase assay was performed using recombinant MT13-N or MT13-C as enzymes, recombinant human eEF1A1 as the substrate and [^{3}H]-AdoMet (PerkinElmer) as the methyl donor. Methyltransferase reactions were set-up on ice in storage buffer, containing 1 µg of recombinant MT13-N or MT-13C, 1 µg of recombinant human eEF1A1, and 0.5 µCi of [^{3}H]-AdoMet in a total volume of 10 µl. The reactions were incubated for 1 hour at 30°C. Proteins were separated by size using SDS-PAGE, transferred to a polyvinylidene difluoride membrane (Millipore, IPVH00010), and stained with Ponceau S. Fluorography was performed to visualize the incorporation of tritium-labeled methyl groups into proteins. The membrane was dried, sprayed with EN3HANCE spray (Perkin-Elmer) and exposed to Kodak BioMax MS film (Sigma-Aldrich) at −80°C, for 1–30 days. Precision Plus Protein Dual Color Standards (Bio-Rad) was used to evaluate the size of polypeptides after SDS-PAGE, and Glow Writer autoradiography pen (Sigma-Aldrich) was used to mark the position of the standards on PVDF membrane, enabling their visualization by fluorography. All fluorography experiments were performed three times.

Enrichment of EEF-1A from nematode extracts

Wild-type and *metl-13(tm6870)* animals were grown on 15 cm^2 NGM agar plates seeded with *E. coli* OP50 at 20°C. A mix of embryos, larvae, and adults were washed off the plates with 1x M9 buffer and transferred to a 15 ml conical tube. The collected animals were washed thrice in 1x M9 buffer by letting them sink to the bottom of the tube for 10 minutes and removing the supernatant. The animals were transferred to a 1.5 ml microcentrifuge tube and further pelleted by centrifugation at 3,000 rcf for 1 minute. Afterwards, the supernatant was removed and pelleted animals were snap-

frozen in liquid nitrogen. Pellets were ground into a fine powder and lysed for 30 minutes at 4°C in lysis buffer [50 mM Tris-HCl pH 7.4, 100 mM NaCl, 1% Triton X-100, 5% glycerol (w/vol), 5 mg/ml Complete™ protease inhibitor cocktail (Roche), 1% P8340 (Sigma)]. Lysates were cleared by centrifugation at 16,100 rcf for 5 minutes at 4°C, and the subsequential enrichment of EEF-1A protein by cation exchange was performed at 4°C. Cleared lysates were loaded on with lysis buffer pre-equilibrated Pierce Strong Cation Exchange (S) Spin Columns (Thermo Fisher Scientific) and centrifugated at 2,000 rcf for 5 minutes. The column was washed twice with washing buffer [50 mM Tris-HCl pH 7.4, 150 mM NaCl, 5% glycerol (w/vol), 5 mg/ml Complete™ protease inhibitor cocktail (Roche), 1% P8340 (Sigma)]. Bound proteins were eluted from the column with elution buffer [50 mM Tris-HCl pH 7.4, 400 mM NaCl, 5% glycerol (w/vol), 5 mg/ml Complete™ protease inhibitor cocktail (Roche), 1% P8340 (Sigma)]. SDS-PAGE samples were prepared from the whole eluate as previously described.

Mass spectrometry

Samples deriving from wild-type or *metl-13(tm6870)* animals were enriched for EEF-1A as described previously and resolved by SDS-PAGE. Protein gels were stained with Coomassie Blue solution [0.2% (w/v) Coomassie Blue, 7.5% (v/v) acetic acid, 50% (v/v) ethanol], and a band corresponding to the mass of EEF-1A (~ 50 kDa) was excised from the gel and cut into 8 pieces before being moved to a 1.5 ml microcentrifuge tube. In-gel digestion was performed on gel pieces containing EEF-1A via the use of chymotrypsin or Glu-C and the resulting fragments were desalted with the use of 10 µl OMIX C18 micro-SPE pipette tips (Agilent). The samples were analyzed by nanoLC-MS using either an Ultimate 3000 RSLCnano-UHPLC system connected to a Q Exactive mass spectrometer (Thermo Fisher Scientific) or a NanoElute-UHPLC coupled to a TimsTOF Pro mass spectrometer (Bruker Daltonics). The resulting LC-MS data were analyzed by searching against the *C.* elegans protein sequence database from Swiss-Prot (4155 entries) with Peaks Studio version 10.6 (Bioinformatics Solution Inc.). The maximum number of variable modifications on a peptide was restricted to three, allowing the following variable modifications: cysteine propionamidation, methionine oxidation, methylation of lysine (mono, di, and tri), and methylation of the N-terminus (mono, di, and tri). MS/MS spectra of the EEF-1A

peptides encompassing N-terminal G2 or K55 were assessed for presence or absence of methylated residues. The methylation status of G2 and K55 on EEF-1A was estimated by the relative signal intensity for each methylated species (unmethylated, mono-, di-, or trimethylated) using Peaks Studio from two biological replicates. Proteomics data for one biological replicate of each sample have been deposited to the ProteomeXchange Consortium via the PRIDE partner repository with the dataset identifier PXD042540 and 10.6019/PXD042540[100].

SUnSET assay

Synchronous arrested L1 larvae from wild-type and *metl-13(tm6870)* animals were obtained by bleaching gravid adults. A total of 16,000 L1 larvae per strain were grown on NGM plates seeded with *E. coli* OP50 bacteria for each biological replicate. Once the young adult stage was reached, the animals were collected from the plates with 1x S-basal [100 mM NaCl, 50 mM KH_2PO_4, 5 mg cholesterol] and transferred to a 15 ml conical tube. The animals were washed twice in 1x S-basal by centrifugation at 1,500 rpm for 1 minute followed by aspiration of the supernatant. Pelleted animals were resuspended in 4 ml of 1x S-basal and moved to a 50 ml Erlenmeyer before being supplemented with 750 µl of a 10x concentrated *E. coli* OP50 culture and 250 µl puromycin (P8833, Sigma) dissolved in ethanol (10 mg/ml). Puromycin treatment was carried out for 4 hours at 200 rpm. Negative controls for the puromycin treatment were prepared similarly, except for the addition of 250 µl ethanol instead of puromycin stock solution. Animals that were treated with or without puromycin were collected in a 15 ml conical tube and pelleted by centrifugation at 1,500 rpm for 1 minute. The supernatant was removed and the collected samples were snap-frozen in liquid nitrogen before preparing lysates. Three micrograms of total protein were loaded per well for western blot analysis. The presence of peptides containing puromycin and actin were detected by anti-puromycin (Merck, MABE343) antibodies (1:5000 dilution), and anti-actin (Abcam, ab8227) antibodies (1:5000 dilution), respectively. Relative puromycin signal was calculated by normalizing to actin expression for three biological replicates.

RNA interference

RNAi was utilized for post-transcriptional gene silencing. Gene-specific RNAi was achieved by feeding the animals *E. coli* HT115 bacteria carrying the L4440 plasmid expressing dsRNA complementary to a gene of interest. All bacterial RNAi clones used in this research derived from the Ahringer library and were verified by Sanger sequencing. *E. coli* HT115 bacteria carrying an empty L4440 plasmid were used as a mock control[73,101]. Bacterial RNAi clones of interest were inoculated in LB medium supplemented with 50 µg/ml carbenicillin and incubated for 16 hours at 37°C, 200 rpm. Bacteria were induced with 1 mM IPTG and incubated for an additional hour before seeding 250 µl on 6 cm^2 RNAi plates [0.25% (w/v) tryptone, 0.3% (w/v) NaCl, 1.5% (w/v) agar, 1 mM $CaCl_2$, 1 mM $MgSO_4$, 25 mM KPO_4 pH 6.0, 5 µg/mL cholesterol, 50 µg/ml carbenicillin, 1 mM IPTG]. Synchronized L1 larvae were plated out on air-dried RNAi plates and grown at 25°C until reaching the 1-day adult stage.

Microscopy

Slides were prepared by anesthetizing animals in a drop of 10 mM levamisole on a 2% (w/v) agarose pad and covering with a cover slip. Animals were immediately imaged with the AxioImager Z1 microscope (Zeiss). The differential interference contrast (DIC) channel was used for all experiments and the green fluorescence protein (GFP) channel was used for imaging LIN-41::GFP expression. Images were acquired via the Axiocam MRm REV2 CCD camera and the Zen software (Zeiss). All acquired images were processed with ImageJ.

Development and fecundity assays

Synchronous arrested L1 larvae from wild-type and *metl-13(tm6870)* animals were obtained by bleaching gravid adults. Approximately 30 animals were plated out on NGM agar plates seeded with *E. coli* OP50 and grown at 25°C for 24 hours. After reaching the L4 larval stage, animals were singled onto separate plates (counted as day 0) and grown at either 25°C, 20°C, or 15°C. The parental animal was moved to a new plate every 24 hours and plates with progeny were kept for counting progeny. In order to get an insight into larval developmental times between the two strains, the offspring were counted and removed every 24 hours after reaching the L4 larval stage. Differences in animal fecundity between the two strains were determined by comparison of total progeny.

Body area measurements

Synchronous arrested L1 larvae from wild-type and *metl-13(tm6870)* animals were obtained by bleaching gravid adults. A minimum of 50 animals were plated out on NGM plates seeded with either *E. coli* OP50 or *E. coli* HB101 and grown at 25°C until the 1-day old adult stage. Microscopy slides of the animals were prepared and micrographs depicting whole animals were obtained using the AxioImager Z1 microscope (Zeiss). The body area of a minimum of 15 animals was measured in square pixels with ImageJ for each biological replicate.

Egg-to-egg assay

The egg-to-egg assay was used to measure the time it takes for an animal to develop from an egg into an adult that starts laying eggs. The egg-to-egg assay was used to compare wild-type and *metl-13(tm6870)* development on an *E. coli* OP50 and *E. coli* HB101 diet. For this assay, four gravid animals were moved to a 6 cm^2 NGM agar plate seeded with either *E. coli* OP50 or *E. coli* HB101 to lay eggs for 2 hours at 25°C before being removed from the plate. The offspring was kept at 25°C until reaching the L4 stage before being picked over onto separate NGM agar plates seeded with the same bacterial food-source. The animals were kept at 25°C and checked every hour once reaching adulthood to mark the time they laid their first egg. A minimum of 20 animals were assessed for each biological replicate.

Lifespan assay

Synchronous arrested L1 larvae from wild-type, *metl-13(tm6870)*, and *eef-1A.1(syb2837); eef-1A.2(syb2785)* animals were obtained by bleaching gravid adults. Animals were plated out per 6 cm^2 NGM agar plate seeded with *E. coli* OP50 and grown at 20°C until the young adult stage, which is day 0 of the lifespan assay. The population was moved to a fresh plate every 24 hours during fertile adulthood in order to omit progeny from the assay, afterwards, the population was moved every 3 days to avoid starvation. Animals were considered dead when not responding to touch by a worm pick, dead animals were counted and removed from the plate every 48 hours. Lifespan was assessed with a minimum of a 100 animals per biological replicate.

Cold lifespan assay

Synchronous arrested L1 larvae from wild-type, *metl-13(tm6870)*, and *rege-1(rrr13)* animals were obtained by bleaching gravid adults. A minimum of 100 animals were plated out per 6 cm^2 NGM agar plate seeded with *E. coli* OP50 and grown at 20°C until the animals were 1-day old adults, which is day 0 of the cold lifespan assay. Animals were adapted to the cold by incubation at 10°C for 2 hours before shifting to 4°C. At each time point, the animals were shifted back to 20°C to recover for 24 hours prior to counting live and dead animals. Animals were considered dead when unresponsive to being touched by a worm pick. A minimum of 100 animals were assessed per biological replicate.

Heat shock assay

Synchronous arrested L1 larvae from wild-type and *metl-13(tm6870)* animals were obtained by bleaching gravid adults. A minimum of 100 animals were plated out per 6 cm^2 NGM agar plate seeded with *E. coli* OP50 and grown at 25°C until the L4 stage. The heat shock was applied by shifting animals to 37°C for 2 or 2.5 hours. Animals were grown for 16 hours at 20°C to recover prior to counting live and dead animals. Animals were considered dead when unresponsive to being touched by a worm pick. A minimum of 100 animals were assessed per biological replicate.

Results

The biochemical function of METTL13 is conserved between humans and *C. elegans in vitro*

The *C. elegans* gene C01B10.8, further referred to as *metl-13*, is an ortholog of human *METTL13* and encodes the METL-13 protein. Human and nematode METTL13/METL-13 are homologous in their sequence (33% identical) and their domain arrangement, with an N- and C-terminal 7BS MTase-like domain separated by a linker region (**Figure 9A**). For the human protein, it is known that the N-terminal KMT-like MTase domain of METTL13 dimethylates eEF1A at K55 (eEF1A^{K55me2}) and the C-terminal SpdS-like MTase domain trimethylates the α-amino group at G2 (eEF1A^{G2me3}) after the removal of the initiator methionine[47]. In order to assess if this methylation activity is conserved in the nematode, we expressed and purified from *E. coli* fragments of METL-13 containing the individual putative MTase domains (MT13-C and MT13-N) with an N-terminal histidine (His) tag (**Figure 9A**). The *C. elegans* (*Ce*) MT13-C and MT13-N fragments were separately assessed in an *in vitro* methyltransferase assay, using [^{3}H]-AdoMet as a methyl donor and recombinant His-tagged human (*Hs*) eEF1A as a protein substrate. Following incubation of the reaction mixture and SDS-PAGE, [^{3}H]-methylated eEF1A was detected by fluorography as a distinct band. We observed that MT13-C methylates eEF1A carrying a C-terminal His-tag, but not an N-terminal His-tag, suggesting the specificity for the N-terminus. This was confirmed when MT13-C dependent methylation was abolished in an eEF1A G2I mutant carrying a C-terminal His-tag. The MT13-N fragment is able to methylate eEF1A independent of the His-tag placement, but methylation was abolished in an eEF1A K55R mutant, pointing to K55 as the key methylation site for MT13-N. Furthermore, MT13-C and MT13-N fragments containing a point mutation in motif post I, which are assumed to be essential for AdoMet binding, were no longer able to methylate eEF1A (**Figure 9D-F**)[102]. Altogether, these experiments indicate that the enzymatic activity of METL-13 matches that of the human METTL13 *in vitro*, with the C-terminal domain of METL-13 methylating eEF1A on G2 and the N-terminal domain methylating K55.

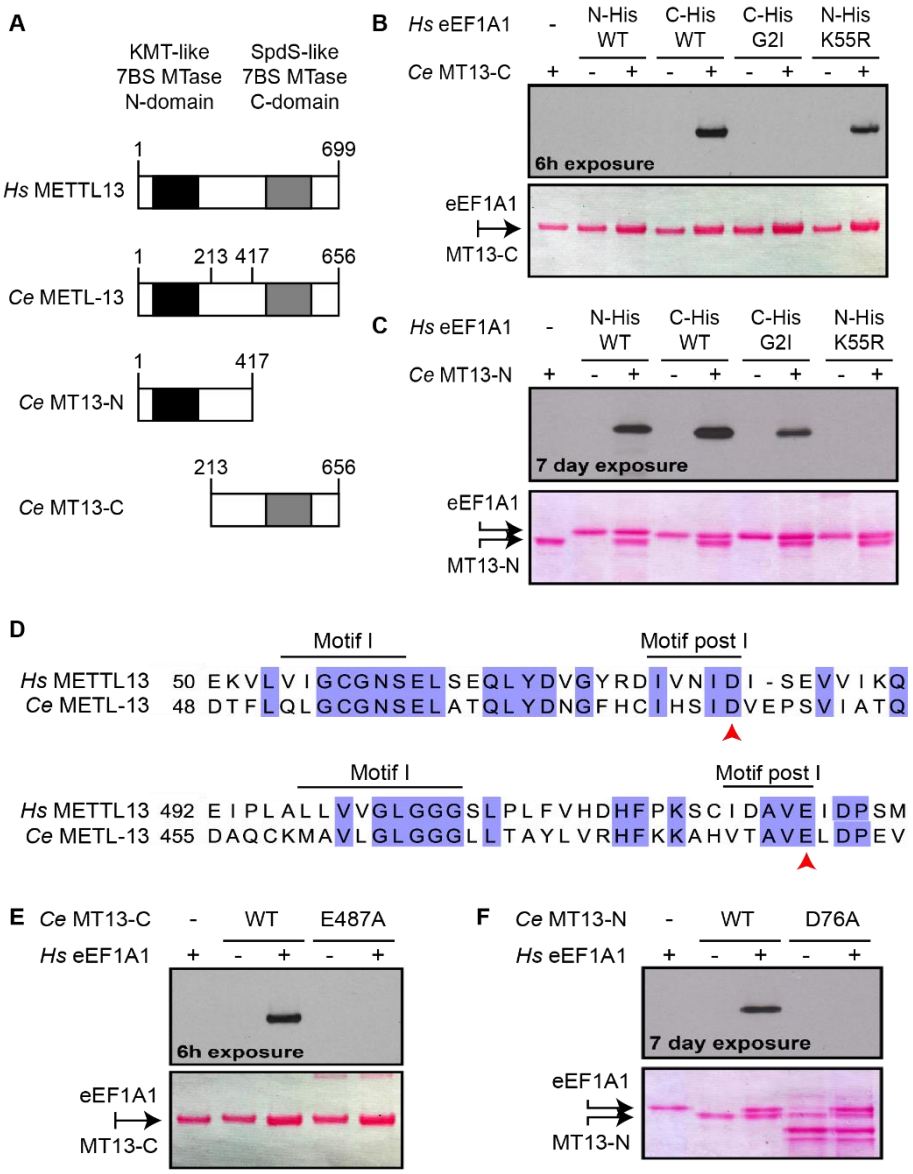

Figure 9: *C. elegans* METL-13 can methylate human eEF1A1 at K55 and G2 *in vitro*. A) Schematic depiction of the domain architecture of full-length human and *C. elegans* METTL13/METL-13 and recombinant METL-13 fragments MT13-N and MT13-C, which were used during the *in vitro* MTase assays. **B,C)** Evaluation of the MTase activity *in vitro* of *C. elegans* METL-13 fragments using recombinant human eEF1A1 as a substrate. MT13-C (**B**) and MT13-N (**C**) were incubated with [^{3}H]-AdoMet and N- or C-terminally His-tagged eEF1A1 in its WT form or carrying point substitutions (G2I or K55R). Methylation was assessed by fluorography (top panels) and protein loading by Ponceau S staining (bottom panels). **D)** Alignment of human and *C. elegans* METTL13/METL-13 covering motifs I and post I in the N-terminal (top) and the C-terminal MTase domain (bottom). Red arrowheads point to a residue in motif post I that is suggested to be necessary for 7BS MTases to interact with AdoMet. **E,F)** The MTase activities of MT13-C and MT13-N are abolished when substituting the last residue in motif post I to alanine. *In vitro* MTase assays were set-up and assessed similarly to **B** and

C, using C-terminally His-tagged human eEF1A1 as a substrate and MT13-C in its WT form or carrying a E487A substitution (**E**), or MT13-N that is either WT or carrying a D76A substitution (**F**). Image is adapted from Engelfriet, et al., 2023[56].

In vivo validation of the biochemical function of METL-13

In order to assess if METL-13 functions as a dual MTase *in vivo*, we utilized a previously uncharacterized mutant strain named *metl-13(tm6870)*. This mutant strain carries a homozygous deletion in *metl-13*, leading to a frameshift in exon 3 and finally resulting in a premature stop codon (**Figure 10A**). Suspecting that mRNA of this mutant *metl-13* would be degraded through non-sense mediated mRNA decay, we assessed the transcript expression of *metl-13* via RT-qPCR. Indeed, *metl-13* mRNA levels were significantly lower in *metl-13(tm6870)* animals compared to wt (**Figure 10B**). Additionally, the hypothetical METL-13 protein from these mutant transcripts should completely lack the C-terminal MTase domain as well as part of the N-terminal MTase domain.

Due to a duplication event during evolution, *C. elegans* contains two genes encoding eEF1A: *eef-1A.1* and *eef-1A.2*[103]. Although the genes slightly differ in sequence (94% identical), the encoded protein (EEF-1A) is identical and is well conserved to human eEF1A around the G2 and K55 residues (**Figure 10C**). To establish if the methylation state of G2 and K55 is conserved in the nematode and whether this methylation is dependent on METL-13, we assessed endogenous eEF1A from wt and *metl-13(tm6870)* animals by MS. Peptides corresponding to EEF-1A were found to be fully trimethylated at G2 and almost completely (99.6%) dimethylated at K55 in wt animals, showcasing that these methylation sites are conserved between humans and *C. elegans* (**Figure 10D,E**). In contrast, neither of the methylation marks were detected on EEF-1A derived from *metl-13(tm6870)* animals (**Figure 10D,E**). Altogether, we found that METTL13 attributed methylation events on eEF1A are conserved in the nematode.

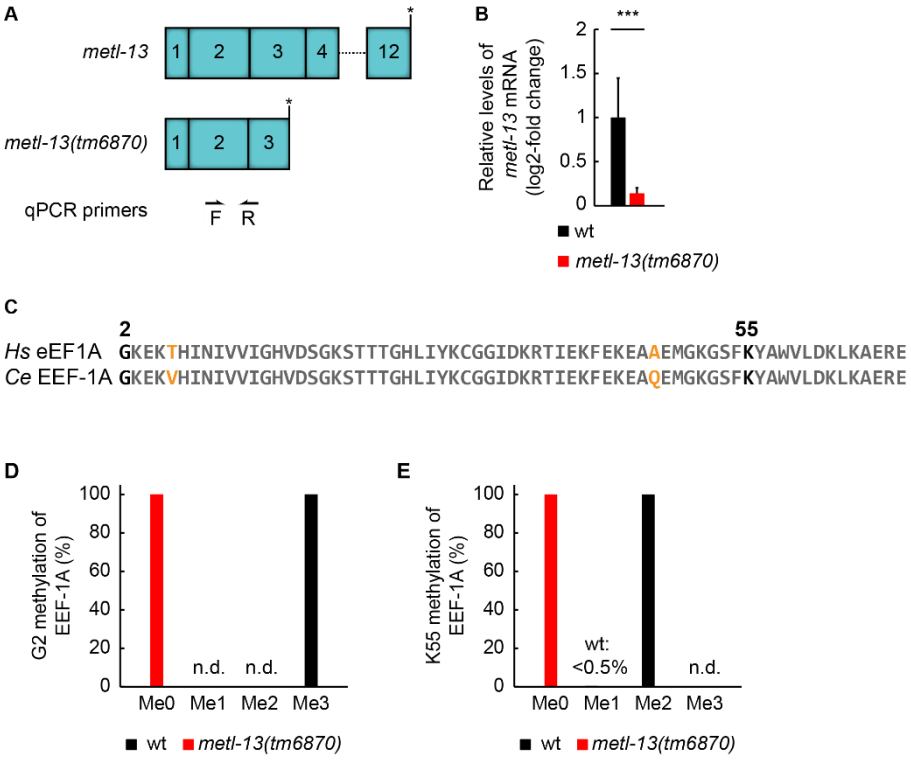

Figure 10: The methylation marks on G2 and K55 on endogenous EEF-1A are conserved in *C. elegans* and dependent on METL-13. A) Schematic representation showing the wt *metl-13* gene (exons are represented by numbered blue boxes, * indicated the stop codon) and the *metl-13(tm6870)* gene containing a premature stop codon. Annealing sites for the used qPCR primers are indicated by arrows (F: forward, R: reverse). **B)** Partial alignment of human eEF1A and *C. elegans* EEF-1A after cleavage of the initiator methionine. The conserved G2 and K55 residues are indicated in bold, non-conserved residues are colored orange. **D,E)** Quantitative analysis of the methylation state of G2 (**D**) and K55 (**E**) on endogenous EEF-1A from wt or *metl-13(tm6870)* animals. Image is adapted from Engelfriet, et al., 2023[56].

Lack of METL-13-mediated methylation does not affect EEF-1A expression or global protein synthesis

Since eEF1A is described as the only substrate of METTL13, we assessed the potential effect that the METL-13-attributed methylation marks might have on EEF-1A protein levels and function. Analysis of EEF-1A protein expression via western blotting revealed no difference in its levels between wt and *metl-13(tm6870)* animals (**Figure 11A**). Furthermore, we generated a double mutant *eef-1A.1(syb2837); eef-1A.2(syb2785)* strain by CRISPR-Cas9 editing, in which the two genes express EEF-1A with a K55R substitution. Arginine was chosen as it shares physicochemical properties with lysine while blocking METL-13-dependent methylation on EEF-1A at position 55, as seen in our *in vitro* MTase assays (**Figure 9C**)[104]. Analyzing this strain via western blotting revealed that both WT and K55R mutated EEF-1A were expressed similarly (**Figure 11A**). Finally, we asked if METL-13-mediated methylation affects the function of EEF-1A in protein translation. Global protein translation was evaluated in wt and *metl-13(tm6870)* animals using the surface sensing of translation (SUnSET) assay[105,106]. However, no difference was found between animals containing or lacking functional METL-13 (**Figure 11B**). These results indicate that ablation of METL-13 has no consequences on protein expression of EEF-1A or on global translation during standard growth conditions.

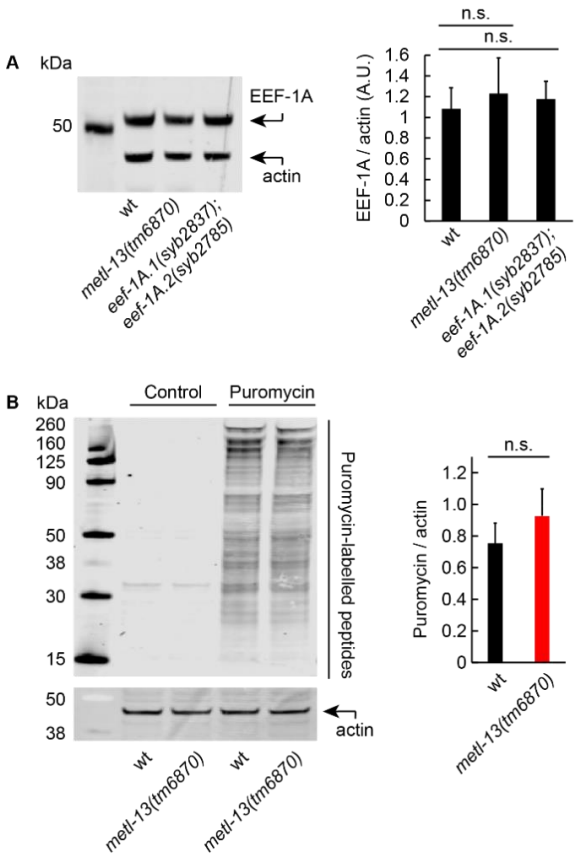

Figure 11: Lack of functional METL-13 or K55me2 on EEF-1A does not affect protein levels of EEF-1A or global protein synthesis. A) Protein levels of EEF-1A remain unchanged in the absence of METL-13 or K55me2. Left: western blot depicts the protein levels of EEF-1A and actin (loading control) in extracts from mixed-stage wt, *metl-13(tm6870)*, or *eef-1A.1(syb2837); eef-1A.2(syb2785)* animals. Right: Densiometric quantification of normalized EEF-1A levels. The error bars indicate the standard error of the mean (SEM) from three biological replicates; n.s.: non-significant. **B)** Global protein synthesis as assessed by SUnSET assay is not affected by ablation of METL-13. Left: western blot depicts the levels of puromycin-labelled peptides and actin (loading control) in extracts from young adult wt and *metl-13(tm6870)* animals. Right: Densiometric quantification of incorporated puromycin levels normalized to actin. The error bars indicate the SEM from three biological replicates; n.s.: non-significant. Image is adapted from Engelfriet, et al., 2023[56].

K55 dimethylation of EEF-1A increases the penetrance of germline tumors

In humans, a link has been established between METTL13-mediated dimethylation of eEF1A on K55 (eEF1A^{K55me2}) and cancer. High levels of METTL13 and eEF1A^{K55me2} correlate with poor survival of patients with lung or pancreatic cancer[55]. In contrast to non-transformed cells, ablation of METTL13 in human cancer cell lines reduces their proliferation and global protein synthesis[55,69]. Since the biochemical function of METL-13 is conserved between humans and *C. elegans*, we wanted to assess its role in tumorigenesis as well. Due to transcription being largely silenced in the germline, RBPs coordinate germ cell proliferation via post-transcriptional regulation of maternally deposited transcripts. Loss-of-function mutations in certain RBPs can cause inappropriate germ cell proliferation that result in the formation of germline tumors, suggesting that these factors could function as tumor suppressors in *C.elegans*[107]. One such RBP is the translational repressor GLD-1[95,108]. In the absence of GLD-1, germ cells that have entered the meiotic pathway return to the mitotic cycle, resulting in a large proximal tumor of ectopically proliferating cells (**Figure 12A**)[94,108,109]. Another example is PRO-1, a WD-repeat protein that plays a role in ribosome biogenesis[110]. Although the etiology of tumorigenesis is less clear in *pro-1* reduction-of-function mutants, the distal germline of these animals contain under proliferated early germ cells, which proliferate ectopically in the proximal germline (**Figure 12A**)[110,111].

In order to evaluate if METL-13 plays a role in germline tumorigenesis in *C. elegans*, we depleted *gld-1* via RNAi in wt animals and *metl-13(tm6870)* mutants. As anticipated, the majority of the gonads in wt animals developed a large proximal tumor containing small undifferentiated cells, a phenotype we will further refer to as 'fully proliferative' (**Figure 12B**). Although this was also observed upon *gld-1* depletion in *metl-13(tm6870)* mutants, it was not the predominant phenotype as in wt animals. In contrast, most of the tumorous gonads of animals lacking functional METL-13 contained enlarged cells reminiscent of differentiating oocytes, a phenotype that we refer to as 'proliferative with enlarged cells' (**Figure 12B and S1A**). Interestingly, this phenotype was also observed in *eef-1A.1(syb2837); eef-1A.2(syb2785)* mutants upon *gld-1* knock down, suggesting that the increase in differentiating cells is due to lack of methylation at K55 on EEF-1A (**Figure 12B and S1A**). When assessing the effect of

non-functional METL-13 in *gld-1(q485)* null mutant animals, we did not observe the same phenotype as seen with *gld-1* RNAi, as all gonads exclusively contained fully proliferative germline tumors (**Figure S2A**). These results could indicate that the absence of METL-13-mediated dimethylation of EEF-1A^{K55} causes less penetrant germline tumors only in the lack but not complete absence of *gld-1*, or that RNAi in these mutant animals is less efficient. To test whether METL-13 or EEF-1A^{K55me2} influence RNAi, we crossed *metl-13(tm6870)* and *eef-1A.1(syb2837); eef-1A.2(syb2785)* animals with a strain that contains transgenic expression of FLAG::GFP::LIN-41 in an endogenous *lin-41(rrr3)* mutant null background. After knocking-down *lin-41* in the FLAG::GFP::LIN-41 expressing strains through RNAi, the expression of FLAG::GFP::LIN-41 in the germline was comparably knocked-down in all strains (**Figure S2B**). Thus, the absence of dimethylated EEF-1A appears to cause less sever germline tumors when GLD-1 expression is reduced but not abolished. In order to further confirm the role of METL-13 in germline tumors, we assessed the effect of METL-13 depletion in the reduction-of-function mutant *pro-1(na48)*, a strain with penetrant tumor formation in the proximal region of the gonads at a restrictive temperature (25°C)[111]. Indeed, most gonads of mock RNAi treated *pro-1(na48)* mutants contained ectopically proliferating germ cells proximal to the gametes, a phenotype we refer to as ‘proximal tumor’ (**Figure 12C**). A minority of these animals contained gonads that lacked a proximal tumor but either appeared wild-type or contained abnormal oocytes, phenotypes which we refer to as ‘wt-like’ or ‘abnormal oocytes’, respectively. Importantly, the number of gonads with the phenotypes ‘wt-like’ or ‘abnormal oocytes’ increased upon *metl-13* RNAi, while the fraction of gonads with a ‘proximal tumor’ phenotype decreased (**Figure 12C and S1B**). Altogether, our results suggest that the METL-13-mediated dimethylation of EEF-1A^{K55me2} enhances tumorigenesis in the nematode.

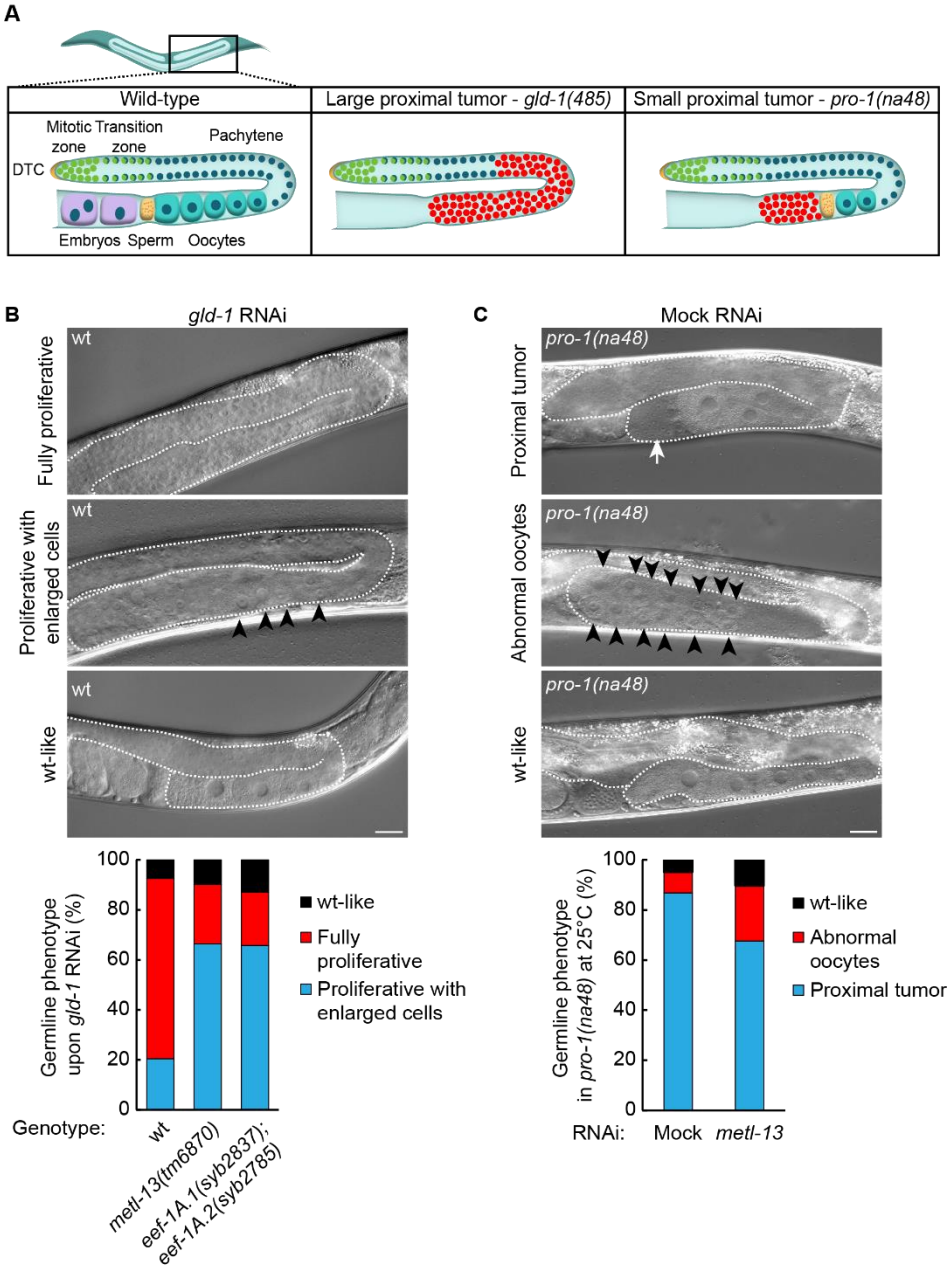

Figure 12: Germline tumors appear less penetrant in animals lacking functional METL-13. A) Schematic depiction of wild-type and tumorous *C. elegans* germlines. The gonads of *gld-1(q485)* null mutants develop large proximal tumors consisting of undifferentiated proliferative germ cells, while those of *pro-1(na48)* loss-of-function mutants develop small tumors proximal to the gametes at a restrictive temperature (25°C). **B)** DIC micrographs of adult wt animals after RNAi knockdown of *gld-1*, the gonads are outlined with a white dotted line; scale bar: 20 µm. One representative micrograph is shown for each of the three phenotypes observed: 'fully proliferative', 'proliferative with enlarged cells' (enlarged cells are indicated by black arrowheads), and 'wt-like'. The bar graph below shows the average distribution of these three phenotypes in wt, *metl-13(tm6870)*, and *eef-1A.1(syb2837); eef-1A.2(syb2785)* animals upon *gld-1* knockdown. The dominant phenotype differs between the

strains, with gonads of wt animals mostly displaying a ‘fully proliferative’ phenotype whereas animals lacking METL-13 or EEF-1A^{K55me2} mostly display a ‘proliferative with enlarged cells’ phenotype. Three biological replicates were used for the quantification, with a minimum of 70 assessed germlines per biological replicate. **C)** DIC micrographs of adult *pro-1(na48)* animals after mock RNAi, the gonads are outlined with a white dotted line; scale bar: 20 µm. One representative micrograph is shown for each of the three phenotypes observed: ‘proximal tumor’ (indicated by a white arrow), ‘abnormal oocytes’ (indicated by black arrowheads), and ‘wt-like’. The bar graph below shows the average distribution of these three phenotypes in *pro-1(na48)* animals upon mock or *metl-13* RNAi. Compared to mock RNAi, knockdown of *metl-13* increased the number of gonads with the ‘abnormal oocytes’ and ‘wt-like’ phenotypes, while less gonads displayed a ‘proximal tumor’ phenotype. Three biological replicates were used for the quantification, with a minimum of 70 assessed germlines per biological replicate. Image from Engelfriet, et al., 2023[56].

METL-13 is non-essential for animal fecundity or development

Since METTL13 has not been studied in depth during normal physiological conditions in whole-animals, we interrogated the potential function of METL-13 in *C. elegans* development and fertility. In order to do so, synchronized L4 wt and *metl-13(tm6870)* animals were singled to individual plates and allowed to grow and lay offspring, which were counted daily after reaching the L4 stage (**Figure 13A**). Since the developmental speed and number of progeny of *C. elegans* depend on temperature, these assays were performed at common laboratory growth temperatures: 15°C, 20°C, and 25°C[112]. We observed no clear difference in the developmental speed or total number of progeny between wt and *metl-13(tm6870)* at all tested temperatures (**Figure 13B**). This indicates that METL-13 is dispensable for development and fertility in *C. elegans* during standard laboratory growth conditions.

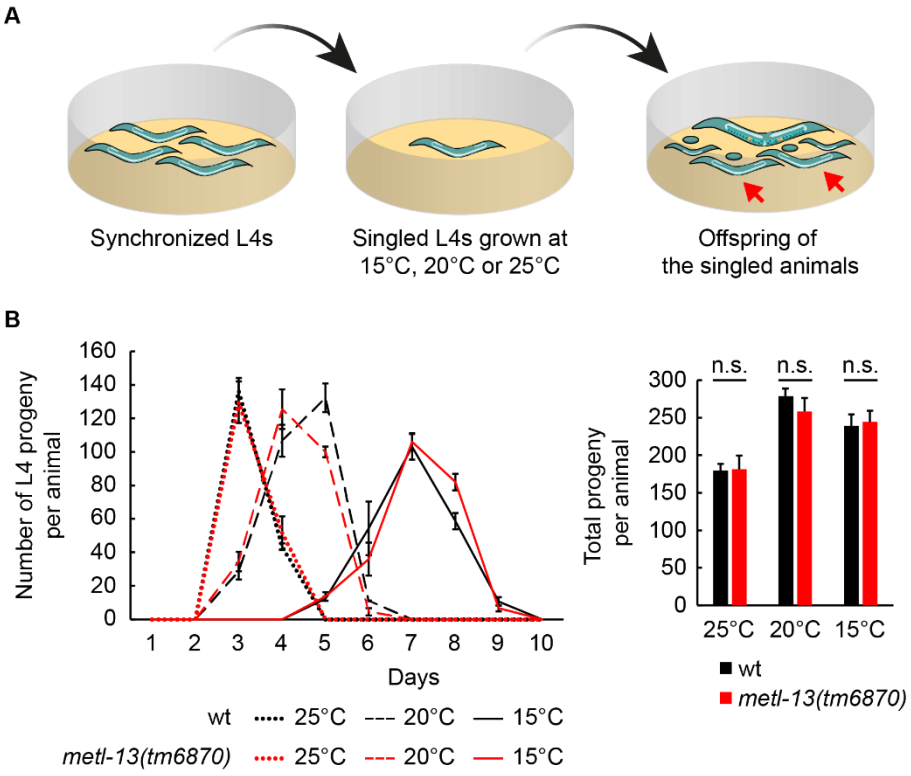

Figure 13: Loss of METL-13 has no clear effect on *C. elegans* development or fecundity during normal growth conditions. A) Schematic representation on how the development and fecundity assays shown were carried out. Synchronized animals were grown to the L4 stage at 20°C, after which animals were singled on separate plates and grown at 15, 20, or 25°C. The offspring of these animals were counted every 24 hours once reaching the L4 stage (red arrows) and removed from the plate. **B)** Developmental speed and fecundity of wt and *metl-13(tm6870)* animals is similar. Left: For the developmental assay, L4 progeny grown at the indicated temperatures were counted every 24 hours. Error bars indicate the SEM from three biological replicates. Right: The graph depicts the total L4 progeny at the indicated temperatures. Error bars indicate the SEM from three biological replicates. Image from Engelfriet, et al., 2023[56].

METL-13 does not impact animal growth under nutrient-rich conditions

Tumorigenesis is linked to increased protein synthesis in order to sustain the uncontrolled growth of cancer cells. Since ablation of METTL13 decreases global protein synthesis specifically in human cancer cell lines, we wondered if other conditions requiring increased protein synthesis could be dependent on METTL13 as well[55,69]. For this purpose, we cultivated wt and *metl-13(tm6870)* mutants on a bacterial diet of *E. coli* HB101 to assess their growth and development. In comparison to the standard *E. coli* OP50 diet, animals that are fed *E. coli* HB101 grow larger and develop faster[71,113–115]. The increase in body size of HB101-fed animals is due to an increase in cell size rather than cell number, which is a consequence of an increase in protein content[115]. To further increase growth and thus demand for protein synthesis, wt and *metl-13(tm6870)* mutants were cultivated at 25°C. The body size of 1-day old adult animals was measured to assay their growth and the time for a laid egg to develop into an egg-laying adult was measured to assess developmental speed. As expected, wt animals grew larger in size and developed faster on a diet of *E. coli* HB101 compared to being fed *E. coli* OP50 (**Figure 14A,B**). However, there was no difference in body size or developmental speed between wt and *metl-13(tm6870*) mutants on either diet (**Figure 14A,B**). Therefore, METL-13 appears to be dispensable for growth and development on a diet of HB101, which demands higher levels of protein synthesis.

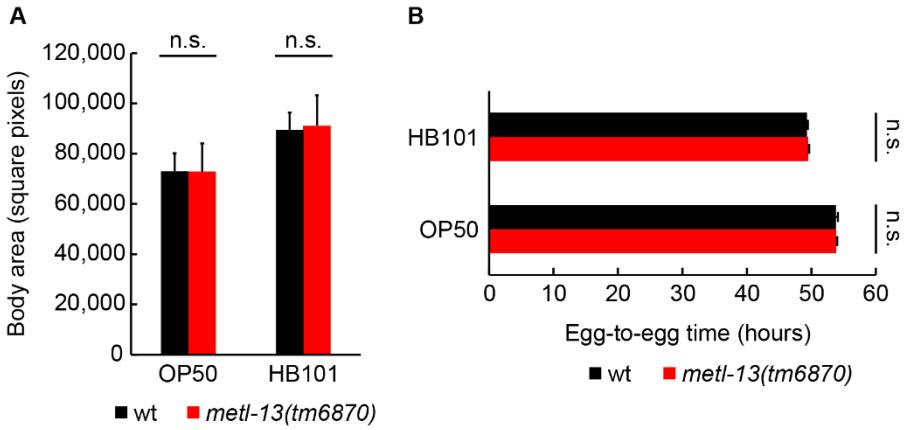

Figure 14: Loss of METL-13 has does not impact growth or development during nutrient-rich conditions. A) The body area 1-day old adult wt and *metl-13(tm6870)* animals was measured after growth at 25°C on a diet or *E. coli* OP50 or HB101. Error bars indicate the SEM of thee biological replicates; n.s.: not significant. **B)** The time for an egg to develop into an egg-laying adult was measured for wt and *metl-13(tm6870)* animals cultivated at 25°C on a diet or *E. coli* OP50 or HB101. Error bars indicate the SEM of thee biological replicates; n.s.: not significant. Image is adapted from Engelfriet, et al., 2023[56].

The absence of METL-13 modestly impairs lifespan independently of K55 dimethylation on EEF-1A

METL-13 is seemingly dispensable for *C. elegans* growth and development under standard growth conditions. Since we only interrogated the role of METL-13 under standard growth conditions during early stages of development, we wondered if it might have a physiological function in the nematode later on in life. In order to get an insight, we assayed the lifespan of animals with or without functional METL-13. Curiously, *metl-13(tm6870)* mutants died a little faster compared to wt animals (**Figure 15**). However, this small but significant decrease in longevity was not observed for *eef-1A.1(syb2837); eef-1A.2(syb2785)* double mutants (**Figure 15**). This suggests that METL-13 plays a modest role in longevity that is unrelated to the methylation status of K55 on EEF-1A.

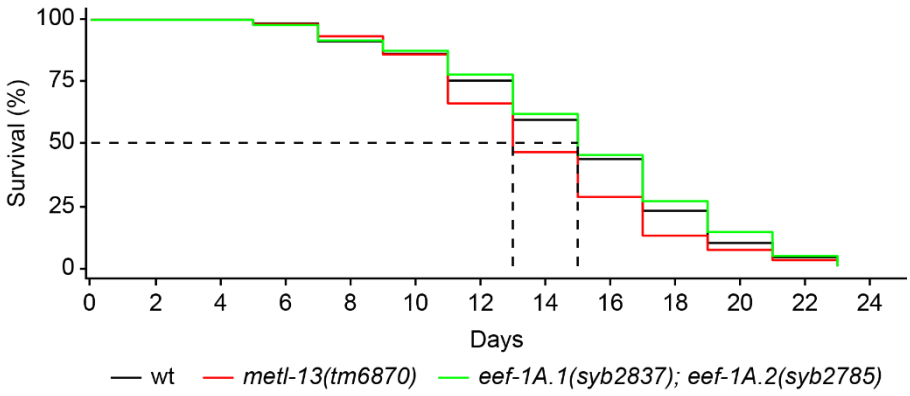

Figure 15: Lack of functional METL-13 negatively impacts longevity independently of K55 methylation on EEF-1A. The lifespan assay was performed at 20°C, using three biological replicates consisting of a minimum of 100 animals per strain, per replicate. P-value wt vs. *metl-13(tm6870)*: 0.024; p-value wt vs. *eef-1A.1(syb2837); eef-1A.2(syb2785)*: 0.43, log-rank test. Image from Engelfriet, et al., 2023[56].

METL-13 does not affect the animals when challenged with cold of heat stress

As *C. elegans* lives in a varied environment in the wild, it must constantly adapt to different environmental stressors. These stressors, such as hazardous temperatures, cause proteins to unfold, misfold, and aggregate, challenging cellular proteostasis[116,117]. Several stress responses, including the unfolded protein response in the endoplasmic reticulum (UPR^{ER}) and the heat-shock response (HSR), are activated during adverse temperatures in order to reduce the levels of misfolded proteins[118,119]. One result of these stress responses is the inhibition of global translation, which reduces the burden on the protein folding machinery[120]. While inhibition of translation initiation plays a key role in the stress-induced decrease in protein synthesis, proteotoxic stressors have also been found to trigger global pausing of translation elongation in order to maintain proteostasis[121,122]. Since METTL13 is known to mediate translation rates of eEF1A, we wondered if it could regulate translation elongation during conditions that impact proteostasis[47]. For this purpose, we assessed the survival of wild-type, *metl-13(tm6870)*, and *rege-1(rrr13)* loss-of-function mutant animals at 4°C after cold adaptation at 10°C for 2 hours. As expected, animals survived less well when containing a deletion in *rege-1*, which normally encodes a ribonuclease known to mediate cold resistance, but the absence of functional METL-13 did not render the animals more or less resistant to the cold (**Figure 16A**)[123]. Similar to cold, a hazardous increase in temperature also challenges *C. elegans* survival. Acute heat shock at 37°C for 2 hours led to a 90% survival rate in wild-type animals, which decreased to 64% when prolonging the heat shock to 2.5 hours (**Figure 16B**). This heat shock-dependent lethality was similar in animals lacking METL-13 (**Figure 16B**). This indicates that METL-13 is not essential in mediating responses to acute or gradual changes in environmental temperature that would challenge proteostasis.

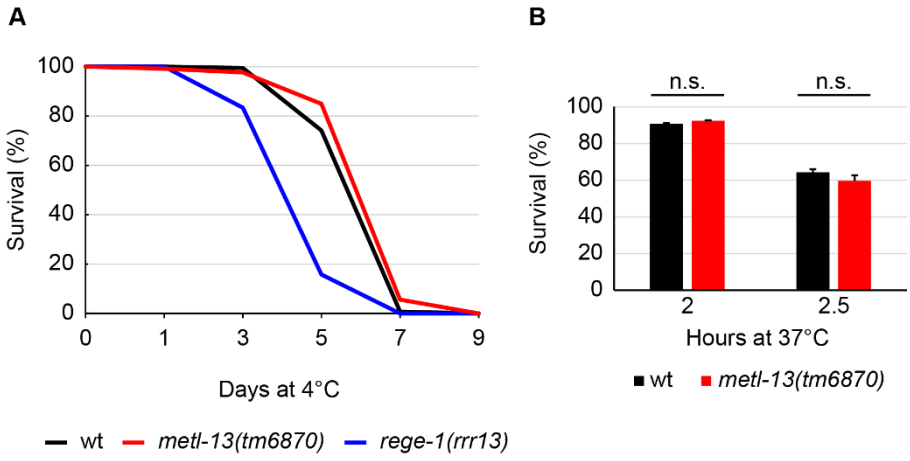

Figure 16: Absence of METL-13 does not affect temperature dependent stress survival in *C. elegans*. A) Cold survival (4°C) is similar between wt and *metl-13(tm6870)* animals and decreased in *rege-1(rrr13)* animals. The survival curve is representative of one biological replicate, with a minimum of 100 assessed animal for each strain at each time point. **B)** Survival of animals after 2 or 2.5 hours of heat stress (37°C) is not affected by a lack of METL-13. Error bars indicate the SEM of three biological replicates; n.s.: not significant.

Discussion

Biochemical characterization of METL-13

Human METTL13 is known to specifically target eEF1A at two residues, trimethylating the N-terminal G2 residue and dimethylating K55[47,55]. In the work underlying this thesis, we studied *C. elegans* METL-13, the previously uncharacterized putative ortholog of human METTL13. We therefore initially set-out to establish if the biochemical function of METL-13 is conserved from human to nematode. Via MTase assays, we found that the human eEF1A1 is methylated *in vitro* at the same positions by *C. elegans* METL-13 MTase domains, with MT13-C targeting G2 and MT13-N K55, underscoring the functional conservation of this dual MTase throughout evolution. While eEF1A is highly conserved, the conservation of certain methylation sites in eukaryotes is not clear[51]. Some methylations on eEF1A orthologs in eukaryotes may not have been identified as of yet, however, the methylation sites on human and yeast eEF1A are most likely completely mapped. In these species, N-terminal trimethylation is conserved but no methylation of K55 is not found in yeast[51] . Reassuringly, we found via mass spectrometry that the G2 and K55 methylation sites are conserved on *C. elegans* EEF-1A, with the former being fully trimethylated and the latter almost fully dimethylated. Importantly, these methylation marks are completely abolished on the endogenous EEF-1A derived from *metl-13(tm6870)* mutant animals that lack functional METL-13, suggesting they are dependent on this dual MTase.

METL-13 substrate specificity

METL-13 appears to be the sole enzyme responsible for the G2 and K55 methylation marks on EEF-1A, but could this enzyme target more potential substrates? For instance, the only other MTases that can methylate the N-terminus of proteins, NTMT1 and NTMT2, are known to target a broad range of substrates containing a [X]-[P]-[K/R] (X = G/S/P/A) consensus motif[18,45]. The C-terminal domain of METTL13 was found to display MTase activity *in vitro* towards a [G/A/P]-[K/R/F/Y/Q/H]-[E]-[K/R/Q/H/I/L] consensus sequence, which makes the existence of multiple *in vivo* substrates for this N-terminal MTase similarly possible[47]. However, from a 15-mer peptide array containing approximately 50 candidate substrates, only the N-terminus of eEF1A was found to be methylated by the C-terminal MTase domain of METTL13[47]. This study suggests that in contrast to other NTMTs, METTL13 is highly specific for the N-

terminus of eEF1A. The specificity of the N-terminal MTase domain of METTL13 for K55 of eEF1A was previously shown by two independent studies through quantitative proteomic screens. In both studies, the methylomes of human cell lines with or without METTL13 were assessed via mass spectrometry, with one focusing on changes in lysine methylation and the other on changes in both arginine and lysine methylation[47,55]. From all lysine and arginine methylation events found in these studies, only dimethylation of K55 on eEF1A was found to be dependent on METTL13[47,55].

While we have shown that the *C. elegans* METL-13 methylates EEF-1A in the same way as has been described in humans, we have not assessed if other substrates might be present in the nematode that are lacking in humans. For instance, the absence of functional METL-13 negatively impacted longevity that was unrelated to dimethylation of EEF-1A^{K55}. This could either implicate a role for EEF-1A^{G2me3} or other unknown METL-13 substrates during ageing in the nematode.

The role of METL-13 in tumorigenesis

Interest in METTL13 has picked up due to the upregulation of the protein itself and the downstream dimethylation of eEF1A^{K55} in a plethora of human cancers[55,58,68,69]. Moreover, targeting METTL13 alleviates cancer cell growth in transformed human cell lines as well as in xenograft and PDAC mouse models[55,69]. This METTL13-dependent effect seems to be mediated specifically through dimethylation of eEF1A^{K55} rather than trimethylation of eEF1A^{G2}, as the proliferation of eEF1A2-depleted cancer cells is rescued by supplementation with the wild-type but not K55R-mutated eEF1A2[55]. Intriguingly, we have found a similar effect in *C. elegans*, when targeting METL-13-mediated dimethylation of K55 on EEF-1A in two genetically induced germline tumors. We observed a decline in the tumor severity when either METL-13 or EEF-1A^{K55me2} were lacking, and that the formation of germline tumors was inhibited but not completely suppressed in the absence of METL-13 or EEF-1A^{K55me2}. This agrees with what has been found in pancreatic and lung PDX tumorous mouse models and human cancer cell lines, where knockdown of METTL13 leads to inhibition but not complete abolishment of tumorous growth[55]. We note that the METL-13-dependent partial suppression was no longer observed in a *gld-1(q485)* null mutants as opposed to *gld-1* knockdown via RNAi. The possibility that the absence of METL-13 or EEF-1A^{K55me2}

could interfere with RNAi was ruled out, as RNAi against a GFP-tagged target was as efficient in these mutant background as in the wild-type. Thus, it appears that abolishing EEF-1A^{K55me2} reduces but not fully blocks tumorigenesis in *gld-1* and *pro-1* hypomorphic tumorous backgrounds. Altogether, we show that METL-13 plays a similar tumor-promoting role as METTL13 and provide a model where the effect of METL-13 and EEF-1A^{K55me2} ablation in a whole animal can be monitored for tumor development.

The impact of eEF1A^{K55me2} on tumorigenesis

Tumorigenesis is negatively affected by a lack of METTL13/METL-13, specifically through a lack of eEF1A^{K55me2}/EEF-1A^{K55me2}. How does this methylation mark benefit cancer? The dimethylation K55 is known to increase the intrinsic GTPase activity of eEF1A *in vitro*, which could lead to increased protein synthesis to meet the demands of a growing tumor[55]. Indeed, global translation in transformed cell lines is reduced upon depletion of METTL13[55,69]. This is in contrast to similar experiments in non-transformed cell lines and our *metl-13(tm6870)* mutant animals, where protein synthesis appears not to be affected[55]. Compared to other components of the translation machinery, eEF1A is present in excess and thus unlikely to be rate-limiting for protein synthesis[124]. However, the translational capacity could be in excess in healthy cells but could become restrictive for protein synthesis upon tumorigenic transformation. Consistent with this, mice haploinsufficient for the eukaryotic translation initiation factor 4E were found to be more resistant to oncogenic transformation while their normal development and protein synthesis was unaffected[125]. This paradigm could be applied to translational elongation as well, as us and others have found that modulation of eEF1A through its dimethylation on K55 is limiting for tumorigenesis but not in normal physiological conditions[55]. As opposed to translation elongation, translation initiation is typically considered to be the rate-limiting step of protein synthesis. The initiation phase during cap-dependent translation relies largely on the ability of the eukaryotic translation initiation factor 4F (eIF4F) complex to bind to the 5'-mRNA cap[126]. Oncogenic pathways can alter the expression, activity, and complex formation of eIF4F members, resulting in increased protein synthesis to sustain tumorous growth[127,128]. While the start of the translation process may be boosted through oncogenic activation of translation initiation, the

translation elongation phase needs to keep up accordingly in order to increase the rate of protein synthesis. In *C. elegans*, it is intriguing that mutations or removal of translational repressors such as GLD-1 leads to the formation of germline tumors. Reducing the presence of GLD-1 causes an increase in translation initiation of the transcripts it would normally repress. This translational output may be reduced upon a lack of METL-13 and EEF-1A^{K55me2}.

Alternatively, non-canonical functions of eEF1A may instead play a role in cancer. Several binding partners of eEF1A were found to have their activity modulated via the interaction with the translation factor during oncogenesis. The activity of sphingosine kinase 1 is upregulated via binding to eEF1A, which has been hypothesized to play a role in oncogenic transformation[129]. Furthermore, the interaction between eEF1A and double-stranded RNA-activated protein kinase hinders its activation as an apoptotic inducer, favoring tumor cells[130]. While the methylation landscape of eEF1A is known to modulate its role in translation elongation, it is not known what role they may play in its moonlighting functions and how this may relate to cancer development.

Targeting METTL13 in cancer therapy

It appears that METTL13 and downstream eEF1A^{K55me2} are only essential for tumorigenic growth, as ablation of METTL13 reduced proliferation and global protein synthesis in human cancer cell lines, but not in non-transformed cell lines[55,69]. This tumor-promoting role of eEF1A^{K55me2} could be inhibited by small molecules, which could be beneficial for the treatment of various cancers. Most therapeutic drugs used in cancer patients target essential proteins such as cell cycle regulators and signaling molecules, causing serious adverse side effects[131–133]. Considering this, the non-essentiality of METTL13 under normal physiological conditions would make a therapeutic drug targeting this enzyme even more of an advantage. However, loss of functional METTL13 has been mostly investigated in the context of cancer as opposed to normal physiology, with all knock-out studies conducted in human cell lines and specific tissues in mice[55,58,69]. Using the *metl-13(tm6870)* mutant strain, we characterized how the loss of METL-13 in a whole-animal affects its growth under physiological conditions. We observed no significant differences between animals with or without functional METL-13 in their development or fecundity. In contrast, animals

lacking METL-13 had a slightly compromised lifespan, indicating that this dual MTase plays a limited but significant role in longevity. Intriguingly, this defect did not phenocopy animals containing the K55R mutation on EEF-1A. Since EEF-1A^{K55me2} was non-essential during normal physiology in the tested assays, but critical for tumorigenesis, our studies endorse the targeting of this modification for cancer therapy.

The impact of METL-13 on longevity

METL-13 appears to play a role in longevity in *C. elegans*, with animals lacking METL-13 but not EEF-1A^{K55me2} alone having a reduced lifespan. This effect could be due to the METL-13-mediated trimethylation of the EEF-1A N-terminus. It could be tested by assessing the lifespan of mutant animals carrying the G2I mutation on EEF-1A, which, according to our *in vitro* MTase assays, would likely prevent METL-13 from trimethylating the N-terminus of EEF-1A. Translation elongation rates are known to decrease during ageing in various animals such as mice, yeast, and *C. elegans*[134,135]. The levels and activity of eEF1A were also found to decline with age in *Drosophila* by ~60%[136]. It is not known if METTL13 could influence eEF1A in ageing animals. Since N-terminal methylation could potentially prevent the degradation of their substrate via the N-degron pathway, the trimethylation mark of eEF1A may be beneficial perhaps to its stability[137]. Alternatively, the methylation of another substrate or other unknown functions of METL-13 may be involved. In this regard, METTL13 was recently found to interact with NTMT1 *in vitro* and inhibit its methylation activity independent of its own catalytic activity[61]. Interestingly, *NTMT1* knockout mice were found to display premature ageing phenotypes[138]. However, whether METTL13 has a similar noncatalytic function *in vivo* and could influence longevity through regulation of NTMT1 remains to be investigated. What is known about the role of METTL13 in the longevity of other model organisms? In mice, pancreas-specific deletion of *Mettl13* was reported to result in no evident developmental or physiological defects, but these experiments are restricted to METTL13 ablation in a single tissue[55]. In contrast, a study in budding yeast found that additional copies of *Efm7*, the functional homolog of the C-terminal MTase domain of METTL13, led to an increase in lifespan[139]. Similar to METTL13, Efm7 trimethylates G2 at the N-terminus of yeast eEF1A but has also been shown to dimethylate the neighboring K3 residue[48]. Despite both Efm7 and METTL13 being

solely responsible for targeting the N-terminus of eEF1A, they are not closely related by sequence[47,48].

METL-13 and stress responses

Hazardous environmental changes require a rapid response in order for the organism to survive. Proteostasis is commonly challenged in most adverse conditions due to an increase in misfolded and aggregated proteins[116,117]. Various cellular stress responses, such as the UPR^{ER} and HSR, are activated in order to maintain proteostasis[118,119]. This is achieved by various mechanisms, such as the upregulation of chaperones that assist in protein folding, protein degradation, and global repression of protein synthesis[140]. Inhibiting the production of new proteins may reduce the burden on the protein folding machinery while halting gene expression during potentially error-prone conditions. In addition, the energy that would normally be required for a high demanding process such as protein synthesis can instead be diverted to other mechanisms to restore proteostasis. Apart from the inhibition of translation at the initiation phase, ribosomes globally pause during the early stages of the elongation phase under proteotoxic stress conditions[121,122]. While translation elongation is altered in response to stress, it is not clear if eEF1A or its methylations play a role in mediating proteostasis. The absence of METTL13 has been shown to alter the translation rate of specific codons, specifically, histidine codons were translated faster and alanine codons slower[47]. Changes in codon translation rates have similarly been observed upon genetic depletion of other eEF1A-specific MTases[53,54]. This has led to the belief that the methylation landscape of eEF1A could function to fine-tune protein translation. So far, only the methylation of eEF1A on K165 has been shown to be dynamically induced upon ER stress, but the exact benefit to this modification during stress has not been elucidated[53]. Here, we have shown that METL-13 is not essential for cold resistance or the heat shock response, suggesting that the relevant EEF-1A methylations are not beneficial or harmful for *C. elegans* during temperature stressors that would challenge proteostasis. It is worthwhile to note that genetic manipulations that increased longevity have also been associated with increased stress resistance[141,142]. Furthermore, genetic ablation of various factors were found to render animals less resistant to oxidative stress as well as reducing their lifespan under normal conditions[143]. This correlation between longevity and stress has

led to the belief of ageing being an organismal stressor. As METL-13 appears to play a small role in longevity, we cannot exclude a potential role for METL-13 during specific stress contexts.

Conclusions and future perspectives

We have shown that the biochemistry of METTL13 is conserved from human to nematode, with the dual-methyltransferase METL-13 being responsible for trimethylation of G2 and dimethylation of K55 on EEF-1A. Furthermore, the tumor-promoting role of METL-13 and EEF-1A^{K55me2} are similar to what has been described for their human counterparts. By characterizing animals lacking functional METL-13, we found no role for this dual-methyltransferase in development, fertility, or stress-dependent insults to proteostasis. As METL-13 appears to play a small but significant role in longevity that is uncoupled to its EEF-1A^{K55me2} methylation mark, we endorse inhibition of the N-terminal MTase domain of METTL13 as a therapeutic strategy for cancer treatment. Future identification of specific inhibitors for the N-terminal MTase domain of METTL13 would be promising. Since *C. elegans* germline tumors have been rescued in the past by drug approaches after identification of the relevant pathways genetically, METTL13 specific inhibitors could be applied to this model as well[144,145]. Furthermore, since *C. elegans* allows for high-throughput drug screenings, our whole-animal model of non-functional METL-13 may aid in identifying additional compounds for synergistic effects to repress tumorous proliferation[146,147].

Supplementary information

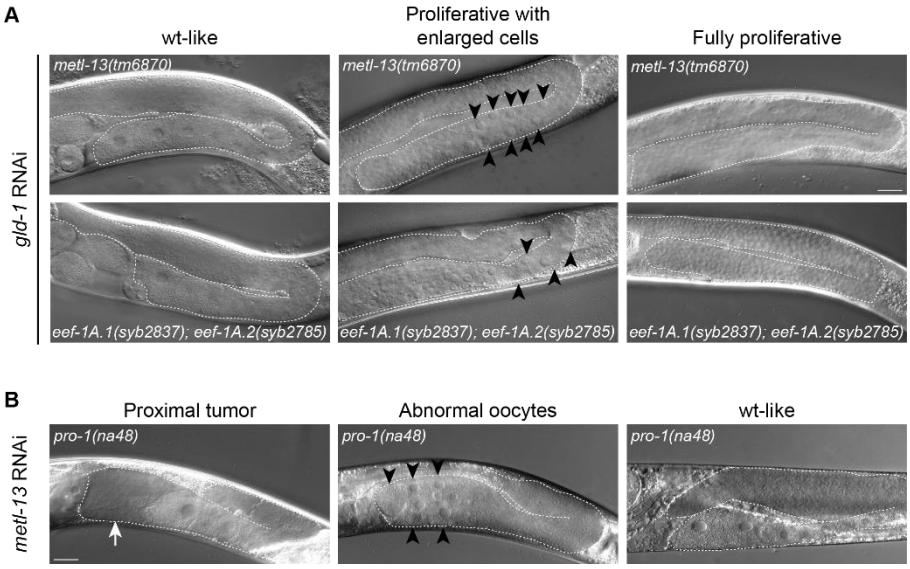

Figure S1: The penetrance of germline tumors is reduced upon depletion of METL-13 or EEF-1A^{K55me2}. A) DIC micrographs of adult *metl-13(tm6870)* and *eef-1A.1(syb2837); eef-1A.2(syb2785)* mutants after RNAi knockdown of *gld-1*, the gonads are outlined with a white dotted line; scale bar: 20 µm. One representative micrograph is shown for each of the three phenotypes observed: 'fully proliferative', 'proliferative with enlarged cells' (enlarged cells are indicated by black arrowheads), and 'wt-like'. **B)** DIC micrographs of adult *pro-1(na48)* animals after RNAi knockdown of *metl-13*, the gonads are outlined with a white dotted line; scale bar: 20 µm. One representative micrograph is shown for each of the three phenotypes observed: 'proximal tumor' (indicated by a white arrow), 'abnormal oocytes' (indicated by black arrowheads), and 'wt-like'. Image from Engelfriet, et al., 2023[56].

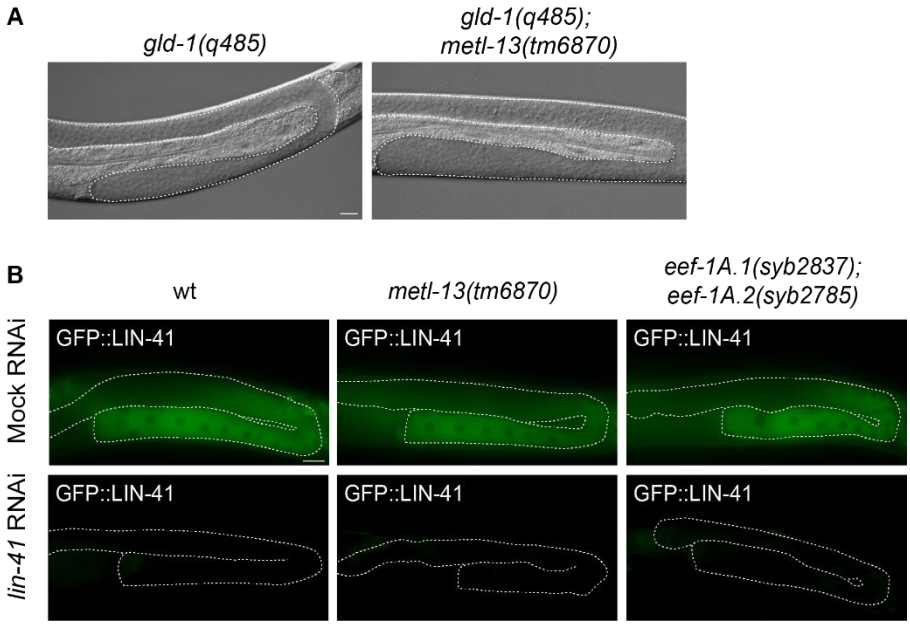

Figure S2: RNAi is as effective in wt animals as in mutants lacking functional METL-13 or EEF-1A^{K55me2}. A) DIC micrographs of adult *gld-1(q485)* null mutant and *gld-1(q485); metl-13(tm6870)* double mutant animals. The gonads of the two mutants both contain large proximal tumors consisting of small proliferative germ cells. The gonads are outlined with a white dotted line; scale bar: 20 µm. **B)** Endogenously expressed GFP::LIN-41 is efficiently and comparably knocked down via RNAi in wt, *metl-13(tm6870)*, and *eef-1A.1(syb2837); eef-1A.2(syb2785)* animals. The gonads are outlined with a white dotted line; scale bar: 20 µm. Image from Engelfriet, et al., 2023[56].

References

1. International Human Genome Sequencing Consortium. Finishing the euchromatic sequence of the human genome. *Nature* **431**, 931–945 (2004).
2. Sulakhe, D. *et al.* Exploring the functional impact of alternative splicing on human protein isoforms using available annotation sources. *Brief. Bioinform.* **20**, 1754–1768 (2019).
3. Aebersold, R. *et al.* How many human proteoforms are there? *Nat. Chem. Biol.* **14**, 206–214 (2018).
4. Ramazi, S. & Zahiri, J. Post-translational modifications in proteins: Resources, tools and prediction methods. *Database* **2021**, 1–20 (2021).
5. Suryadinata, R., Sadowski, M. & Sarcevic, B. Control of cell cycle progression by phosphorylation of cyclin-dependent kinase (CDK) substrates. *Biosci. Rep.* **30**, 243–255 (2010).
6. Zhang, T., Cooper, S. & Brockdorff, N. The interplay of histone modifications – writers that read. *EMBO Rep.* **16**, 1467–1481 (2015).
7. Moore, L. D., Le, T. & Fan, G. DNA methylation and its basic function. *Neuropsychopharmacology* **38**, 23–38 (2013).
8. Zaccara, S., Ries, R. J. & Jaffrey, S. R. Reading, writing and erasing mRNA methylation. *Nat. Rev. Mol. Cell Biol.* **20**, 608–624 (2019).
9. Greer, E. L. & Shi, Y. Histone methylation: A dynamic mark in health, disease and inheritance. *Nat. Rev. Genet.* **13**, 343–357 (2012).
10. Di Blasi, R. *et al.* Non-Histone Protein Methylation: Biological Significance and Bioengineering Potential. *ACS Chem. Biol.* **16**, 238–250 (2021).
11. Vance, D. E. Phospholipid methylation in mammals: From biochemistry to physiological function. *Biochim. Biophys. Acta - Biomembr.* **1838**, 1477–1487 (2014).
12. Ambler, R. P. & Rees, M. W. ε-N-Methyl-lysine in Bacterial Flagellar Protein. *Nature* **184**, 56–57 (1959).
13. Murray, K. The Occurrence of ϵ-N-Methyl Lysine in Histones. *Biochemistry* **3**, 10–15 (1964).
14. Kim, S. & Paik, W. K. Studies on the origin of epsilon-N-methyl-L-lysine in protein. *J. Biol. Chem.* **240**, 4629–4634 (1965).
15. Falnes, P., Małecki, J. M., Herrera, M. C., Bengtsen, M. & Davydova, E. Human seven-β-strand (METTL) methyltransferases - conquering the universe of protein lysine methylation. *J. Biol. Chem.* **299**, 1–15 (2023).

16. Wu, Q., Schapira, M., Arrowsmith, C. H. & Barsyte-Lovejoy, D. Protein arginine methylation: from enigmatic functions to therapeutic targeting. *Nat. Rev. Drug Discov.* **20**, 509–530 (2021).
17. Davydova, E. *et al.* The methyltransferase METTL9 mediates pervasive 1-methylhistidine modification in mammalian proteomes. *Nat. Commun.* **12**, (2021).
18. Diaz, K., Meng, Y. & Huang, R. Past, present, and perspectives of protein N-terminal methylation. *Curr. Opin. Chem. Biol.* **63**, 115–122 (2021).
19. Passos, D. O., Quaresma, A. J. C. & Kobarg, J. The methylation of the C-terminal region of hnRNPQ (NSAP1) is important for its nuclear localization. *Biochem. Biophys. Res. Commun.* **346**, 517–525 (2006).
20. Kapell, S. & Jakobsson, M. E. Large-scale identification of protein histidine methylation in human cells. *NAR Genomics Bioinforma.* **3**, 1–12 (2021).
21. Hamey, J. J. & Wilkins, M. R. The protein methylation network in yeast: A landmark in completeness for a eukaryotic post-translational modification Joshua. *Proc. Natl. Acad. Sci.* **120**, e2215431120 (2023).
22. Abdelraheem, E. *et al.* Methyltransferases: Functions and Applications. *ChemBioChem* **23**, (2022).
23. Petrossian, T. C. & Clarke, S. G. Uncovering the human methyltransferasome. *Mol. Cell. Proteomics* **10**, 1–12 (2011).
24. Petrossian, T. & Clarke, S. Bioinformatic identification of novel methyltransferases. *Epigenomics* **1**, 163–175 (2009).
25. Falnes, P., Jakobsson, M. E., Davydova, E., Ho, A. & Malecki, J. Protein lysine methylation by seven-β-strand methyltransferases. *Biochem. J.* **473**, 1995–2009 (2016).
26. Kagan, R. M. & Clarke, S. Widespread Occurrence of Three Sequence Motifs in Diverse S-Adenosylmethionine-Dependent Methyltransferases Suggests a Common Structure for These Enzymes. *Archives of Biochemistry and Biophysics* vol. 310 417–427 at https://doi.org/10.1006/abbi.1994.1187 (1994).
27. Niewmierzycka, A. & Clarke, S. S-adenosylmethionine-dependent methylation in saccharomyces cerevisiae: Identification of a novel protein arginine methyltransferase. *J. Biol. Chem.* **274**, 814–824 (1999).
28. Martin, J. L. & McMillan, F. M. SAM (dependent) I AM: the S-adenosylmethionine-dependent methyltransferase fold. *Curr. Opin. Struct. Biol.*

12, 783- (2002).

29. Kernstock, S. *et al.* Lysine methylation of VCP by a member of a novel human protein methyltransferase family. *Nat. Commun.* **3**, (2012).
30. Schubert, H. L., Blumenthal, R. M. & Cheng, X. Many paths to methyltransfer: A chronicle of convergence. *Trends Biochem. Sci.* **28**, 329–335 (2003).
31. Feng, Q. *et al.* Methylation of H3-lysine 79 is mediated by a new family of HMTases without a SET domain. *Curr. Biol.* **25**, 1052–1058 (2002).
32. Tschiersch, B. *et al.* The protein encoded by the Drosophila position-effect variegation suppressor gene Su(var)3-9 combines domains of antagonistic regulators of homeotic gene complexes. *EMBO J.* **13**, 3822–3831 (1994).
33. Huang, J. & Berger, S. L. The emerging field of dynamic lysine methylation of non-histone proteins. *Curr. Opin. Genet. Dev.* **18**, 152–158 (2008).
34. Wilkinson, A. W. *et al.* SETD3 is an actin histidine methyltransferase that prevents primary dystocia. *Nature* **565**, 372–376 (2019).
35. Luo, M. Chemical and Biochemical Perspectives of Protein Lysine Methylation. *Chem. Rev.* **118**, 6656–6705 (2018).
36. Roberts, D. M., Rowe, P. M., Siegel, F. L., Lukas, T. J. & Watterson, D. M. Trimethyllysine and protein function. *J. Biol. Chem.* **261**, 1491–1494 (1986).
37. Strahl, B. D., Ohba, R., Cook, R. G. & Allis, C. D. Methylation of histone H3 at lysine 4 is highly conserved and correlates with transcriptionally active nuclei in Tetrahymena. *Proc. Natl. Acad. Sci. U. S. A.* **96**, 14967–14972 (1999).
38. Santos-Rosa, H. *et al.* Active genes are tri-methylated at K4 of histone H3. *Nature* **419**, 407–411 (2002).
39. Bannister, A. J. *et al.* Selective recognition of methylated lysine 9 on histone H3 by the HP1 chromo domain. *Nature* **410**, 120–124 (2001).
40. Lachner, M., O'Carroll, D., Rea, S., Mechtler, K. & Jenuwein T. Methylation of histone H3 lysine 9 creates a binding site for HP1 proteins. *Nature* **410**, (2001).
41. Black, J. C., Van Rechem, C. & Whetstine, J. R. Histone Lysine Methylation Dynamics: Establishment, Regulation, and Biological Impact. *Mol. Cell* **48**, 491–507 (2012).
42. Stock, A., Clarke, S., Clarke, C. & Stock, J. N-terminal methylation of proteins: Structure, function and specificity. *FEBS Lett.* **220**, 8–14 (1987).
43. Chen, R., Brosius, J., Wittmann-Liebold, B. & Schäfer, W. Occurrence of methylated amino acids as N-termini of proteins from Escherichia coli

ribosomes. *J. Mol. Biol.* **111**, 173–181 (1977).

44. Chen, P., Paschoal Sobreira, T. J., Hall, M. C. & Hazbun, T. R. Discovering the N-Terminal Methylome by Repurposing of Proteomic Datasets. *J. Proteome Res.* **20**, 4231–4247 (2021).
45. Dong, C. *et al.* An asparagine/glycine switch governs product specificity of human N-terminal methyltransferase NTMT2. *Commun. Biol.* **1**, 1–9 (2018).
46. Petkowski, J. J. *et al.* Substrate Speci fi city of Mammalian N-Terminal α - Amino Methyltransferase NRMT. (2012).
47. Jakobsson, M. E. *et al.* The dual methyltransferase METTL13 targets N terminus and Lys55 of eEF1A and modulates codon-specific translation rates. *Nat. Commun.* **9**, 3411 (2018).
48. Hamey, J. J. *et al.* Novel N-terminal and lysine methyltransferases that target translation elongation factor 1A in yeast and human. *Mol. Cell. Proteomics* **15**, 164–176 (2016).
49. Kahns, S. *et al. The elongation factor 1 A-2 isoform from rabbit: cloning of the cDNA and characterization of the protein*. *Nucleic Acids Research* vol. 26 (1998).
50. Khalyfa, A. *et al.* Characterization of Elongation Factor-1A (eEF1A-1) and eEF1A-2/S1 Protein Expression in Normal and wasted Mice. *J. Biol. Chem.* **276**, 22915–22922 (2001).
51. Hamey, J. J. & Wilkins, M. R. Methylation of Elongation Factor 1A: Where, Who, and Why? *Trends Biochem. Sci.* **43**, 211–223 (2018).
52. Shimazu, T., Barjau, J., Sohtome, Y., Sodeoka, M. & Shinkai, Y. Selenium-based S-adenosylmethionine analog reveals the mammalian seven-beta-strand methyltransferase METTL10 to be an EF1A1 lysine methyltransferase. *PLoS One* **9**, (2014).
53. Malecki, J. *et al.* The novel lysine specific methyltransferase METTL21B affects mRNA translation through inducible and dynamic methylation of Lys-165 in human eukaryotic elongation factor 1 alpha (eEF1A). *Nucleic Acids Res.* **45**, 4370–4389 (2017).
54. Jakobsson, M. E. *et al.* Methylation of human eukaryotic elongation factor alpha (eEF1A) by a member of a novel protein lysine methyltransferase family modulates mRNA translation. *Nucleic Acids Res.* **45**, 8239–8254 (2017).
55. Liu, S. *et al.* METTL13 Methylation of eEF1A Increases Translational Output to

Promote Tumorigenesis. *Cell* **176**, 491-504.e21 (2019).

56. Engelfriet, M. L., Małecki, J. M., Forsberg, A. F., Falnes, P. & Ciosk, R. Characterization of the biochemical activity and tumor-promoting role of the dual protein methyltransferase METL-13/METTL13 in Caenorhabditis elegans. *PLoS One* **18**, 3–9 (2023).
57. Rhein, V. F., Carroll, J., Ding, S., Fearnley, I. M. & Walker, J. E. Human METTL12 is a mitochondrial methyltransferase that modifies citrate synthase. *FEBS Lett.* **591**, 1641–1652 (2017).
58. Li, L. *et al.* HN1L-mediated transcriptional axis AP-2γ/METTL13/TCF3-ZEB1 drives tumor growth and metastasis in hepatocellular carcinoma. *Cell Death Differ.* **26**, 2268–2283 (2019).
59. Liang, H. *et al.* miR-16 promotes the apoptosis of human cancer cells by targeting FEAT. *BMC Cancer* **15**, (2015).
60. Su, X. F. *et al.* MiR-16 inhibits hepatocellular carcinoma progression by targeting FEAT through NF-κB signaling pathway. *Eur. Rev. Med. Pharmacol. Sci.* **23**, 10274–10282 (2019).
61. Parker, H. & Schaner Tooley, C. Opposing regulation of the Nα-trimethylase METTL11A by its family members METTL11B and METTL13. *J. Biol. Chem.* 104588 (2023) doi:10.1016/j.jbc.2023.104588.
62. Nishi, H., Shaytan, A. & Panchenko, A. R. Physicochemical mechanisms of protein regulation by phosphorylation. *Front. Genet.* **5**, 1–10 (2014).
63. Lecker, S. H., Goldberg, A. L. & Mitch, W. E. Protein degradation by the ubiquitin-proteasome pathway in normal and disease states. *J. Am. Soc. Nephrol.* **17**, 1807–1819 (2006).
64. Geiss-Friedlander, R. & Melchior, F. Concepts in sumoylation: A decade on. *Nat. Rev. Mol. Cell Biol.* **8**, 947–956 (2007).
65. Ulrich, H. D. The Fast-Growing Business of SUMO Chains. *Mol. Cell* **32**, 301–305 (2008).
66. Ikeda, F. & Dikic, I. Atypical ubiquitin chains: New molecular signals. 'Protein Modifications: Beyond the Usual Suspects' Review Series. *EMBO Rep.* **9**, 536–542 (2008).
67. Hornbeck, P. V. *et al.* PhosphoSitePlus, 2014: Mutations, PTMs and recalibrations. *Nucleic Acids Res.* **43**, D512–D520 (2015).
68. Takahashi, A. *et al.* A novel potent tumour promoter aberrantly overexpressed

in most human cancers. *Sci. Rep.* **1**, (2011).

69. Wang, X. *et al.* Methyltransferase like 13 mediates the translation of Snail in head and neck squamous cell carcinoma. *Int. J. Oral Sci.* **13**, (2021).
70. Li, L. *et al.* HN1L-mediated transcriptional axis AP-2γ/METTL13/TCF3-ZEB1 drives tumor growth and metastasis in hepatocellular carcinoma. *Cell Death Differ.* **26**, 2268–2283 (2019).
71. Brenner, S. The genetics of Caenorhabditis elegans. *Genetics* **77**, 71–94 (1974).
72. Frézal, L. & Félix, M. A. C. elegans outside the Petri dish. *Elife* **4**, 1–14 (2015).
73. Kamath, R. S. *et al.* Systematic functional analysis of the Caenorhabditis elegans genome using RNAi. *Nature* **421**, 231–237 (2003).
74. Rual, J. F. *et al.* Toward improving Caenorhabditis elegans phenome mapping with an ORFeome-based RNAi library. *Genome Res.* **14**, 2162–2168 (2004).
75. Equence, C. E. S., Iology, T. O. B., The, C. & Consortium, S. Genome sequence of the nematode C. elegans: A platform for investigating biology. *Science (80-.).* **282**, 2012–2018 (1998).
76. Lai, C. H., Chou, C. Y., Ch'ang, L. Y., Liu, C. S. & Lin, W. C. Identification of novel human genes evolutionarily conserved in Caenorhabditis elegans by comparative proteomics. *Genome Res.* **10**, 703–713 (2000).
77. Silverman, G. A. *et al.* Modeling molecular and cellular aspects of human disease using the nematode Caenorhabditis elegans. *Pediatr. Res.* **65**, 10–18 (2009).
78. Sonnhammer, E. L. L. & Durbin, R. Analysis of protein domain families in Caenorhabditis elegans. *Genomics* **46**, 200–216 (1997).
79. Fire, A. *et al.* Potent and specific genetic interference by double-stranded RNA in Caenorhabditis elegans. *Nature* **391**, 806–811 (1998).
80. Ellis, H. M. & Horvitz, H. R. Genetic Control of Programmed Cell Death in the Nematode C. elegans. *Cell* **44**, 817–829 (1986).
81. Culetto, E. & Sattelle, D. B. A role for Caenorhabditis elegans in understanding the function and interactions of human disease genes. *Hum. Mol. Genet.* **9**, 869–877 (2000).
82. Edgley, M. L., Baillie, D. L., Riddle, D. L. & Rose, A. M. Genetic balancers. *WormBook* 1–32 (2006) doi:10.1895/wormbook.1.89.1.
83. Nurse, P. Fission yeast cell cycle mutants and the logic of eukaryotic cell cycle

control. *Mol. Biol. Cell* **31**, 2871–2873 (2020).

84. Rodriguez, M., Basten Snoek, L., De Bono, M. & Kammenga, J. E. Worms under stress: C. elegans stress response and its relevance to complex human disease and aging. *Trends Genet.* **29**, 367–374 (2013).
85. Hanahan, D. Hallmarks of Cancer: New Dimensions. *Cancer Discov.* **12**, 31–46 (2022).
86. Cerón, J. Caenorhabditis elegans for research on cancer hallmarks . *Dis. Model. Mech.* **16**, (2023).
87. Kopan, R. & Ilagan, M. X. G. The Canonical Notch Signaling Pathway: Unfolding the Activation Mechanism. *Cell* **137**, 216–233 (2009).
88. Chen, J. *et al. GLP-1 Notch-LAG-1 CSL control of the germline stem cell fate is mediated by transcriptional targets lst-1 and sygl-1*. *PLoS Genetics* vol. 16 (2020).
89. Berry, L. W., Westlund, B. & Schedl, T. Germ-line tumor formation caused by activation of glp-1, a Caenorhabditis elegans member of the Notch family of receptors. *Development* **124**, 925–936 (1997).
90. Dalfó, D. *et al.* A genome-wide rnai screen for enhancers of a germline tumor phenotype caused by elevated GLP-1/Notch signaling in caenorhabditis elegans. *G3 Genes, Genomes, Genet.* **10**, 4323–4334 (2020).
91. Marin, V. A. & Evans, T. C. Translational repression of a C. elegans Notch mRNA by the STAR/KH domain protein GLD-1. *Development* **130**, 2623–2632 (2003).
92. Albarqi, M. M. Y. & Ryder, S. P. The role of RNA-binding proteins in orchestrating germline development in Caenorhabditis elegans. *Front. Cell Dev. Biol.* **10**, 1–16 (2023).
93. Crittenden, S. L., Troemel, E. R., Evans, T. C. & Kimble, J. GLP-1 is localized to the mitotic region of the C. elegansgerm line. **120**, 2901–2911 (1994).
94. Biedermann, B. *et al.* Translational Repression of Cyclin E Prevents Precocious Mitosis and Embryonic Gene Activation during C. elegans Meiosis. *Dev. Cell* **17**, 355–364 (2009).
95. Scheckel, C., Gaidatzis, D., Wright, J. E. & Ciosk, R. Genome-wide analysis of GLD-1-mediated mRNA regulation suggests a role in mRNA storage. *PLoS Genet.* **8**, 1–12 (2012).
96. Robichaud, N., Sonenberg, N., Ruggero, D. & Schneider, R. J. Translational

control in cancer. *Cold Spring Harb. Perspect. Biol.* **11**, (2019).

97. Ruggero, D. Translational control in cancer etiology. *Cold Spring Harb. Perspect. Biol.* **5**, a012336 (2013).
98. Knight, J. R. P. *et al.* Control of translation elongation in health and disease. *DMM Dis. Model. Mech.* **13**, (2020).
99. Hodgkin, J. Male Phenotypes and Mating Efficiency in Caenorhabditis Elegans . *Genetics* **103**, 43–64 (1983).
100. Perez-riverol, Y. *et al.* The PRIDE database resources in 2022 : a hub for mass spectrometry-based proteomics evidences. **50**, 543–552 (2022).
101. Fraser, A. G. *et al.* Functional genomic analysis of C. elegans chromosome I by systematic RNA interference. *Nature* **408**, 325–330 (2000).
102. Katz, J. E., Dlakić, M. & Clarke, S. Automated identification of putative methyltransferases from genomic open reading frames. *Mol. Cell. Proteomics* **2**, 525–540 (2003).
103. Maciejowski, J. *et al.* Autosomal genes of autosomal/X-linked duplicated gene pairs and germ-line proliferation in Caenorhabditis elegans. *Genetics* **169**, 1997–2011 (2005).
104. Weirich, S. & Jeltsch, A. Limited choice of natural amino acids as mimetics restricts design of protein lysine methylation studies. *Nat. Commun.* **14**, 14–16 (2023).
105. Schmidt, E. K., Clavarino, G., Ceppi, M. & Pierre, P. SUnSET, a nonradioactive method to monitor protein synthesis. *Nat. Methods* **6**, 275–277 (2009).
106. Arnold, A. *et al.* Functional characterization of C. elegans Y-box-binding proteins reveals tissue-specific functions and a critical role in the formation of polysomes. *Nucleic Acids Res.* **42**, 13353–13369 (2014).
107. Vanden Broek, K., Han, X. & Hansen, D. Redundant mechanisms regulating the proliferation vs. differentiation balance in the C. elegans germline. *Front. Cell Dev. Biol.* **10**, 1–15 (2022).
108. Lee, M. H. & Schedl, T. Identification of in vivo mRNA targets of GLD-1, a maxi-KH motif containing protein required for C. elegans germ cell development. *Genes Dev.* **15**, 2408–2420 (2001).
109. Jones, A. R. & Schedl, T. Mutations in gld-1, a female germ cell-specific tumor suppressor gene in Caenorhabditis elegans, affect a conserved domain also

found in Src- associated protein Sam68. *Genes Dev.* **9**, 1491–1504 (1995).

110. Voutev, R., Killian, D. J., Hyungsoo Ahn, J. & Hubbard, E. J. A. Alterations in ribosome biogenesis cause specific defects in C. elegans hermaphrodite gonadogenesis. *Dev. Biol.* **298**, 45–58 (2006).
111. Killian, D. J. & Hubbard, E. J. A. C. elegans pro-1 activity is required for soma/germline interactions that influence proliferation and differentiation in the germ line. *Development* **131**, 1267–1278 (2004).
112. Byerly, L., Cassada, R. C. & Russell, R. L. The life cycle of the nematode Caenorhabditis elegans: I. Wild-type growth and reproduction. *Dev. Biol.* **51**, 23–33 (1976).
113. Avery, L. & Shtonda, B. B. Food transport in the C. elegans pharynx. *J. Exp. Biol.* **206**, 2441–2457 (2003).
114. Soukas, A. A., Kane, E. A., Carr, C. E., Melo, J. A. & Ruvkun, G. Rictor/TORC2 regulates fat metabolism, feeding, growth, and life span in Caenorhabditis elegans. *Genes Dev.* **23**, 496–511 (2009).
115. So, S., Miyahara, K. & Ohshima, Y. Control of body size in C. elegans dependent on food and insulin/IGF-1 signal. *Genes to Cells* **16**, 639–651 (2011).
116. Vakkayil, K. L. & Hoppe, T. Temperature-Dependent Regulation of Proteostasis and Longevity. *Front. Aging* **3**, 1–6 (2022).
117. Xu, G. *et al.* Vulnerability of newly synthesized proteins to proteostasis stress. *J. Cell Sci.* **129**, 1892–1901 (2016).
118. Le Breton, L. & Mayer, M. P. Heat Shock Response: A model for handling cell stress. *Elife* **5**, (2016).
119. Bettaieb, A. & Averill-Bates, D. A. Thermotolerance induced at a mild temperature of 40°C alleviates heat shock-induced ER stress and apoptosis in HeLa cells. *Biochim. Biophys. Acta - Mol. Cell Res.* **1853**, 52–62 (2015).
120. Holcik, M. & Sonenberg, N. Translational control in stress and apoptosis. *Nat. Rev. Mol. Cell Biol.* **6**, 318–327 (2005).
121. Shalgi, R. *et al.* Widespread Regulation of Translation by Elongation Pausing in Heat Shock. *Mol. Cell* **49**, 439–452 (2013).
122. Liu, B., Han, Y. & Qian, S. B. Cotranslational Response to Proteotoxic Stress by Elongation Pausing of Ribosomes. *Mol. Cell* **49**, 453–463 (2013).
123. Habacher, C. *et al.* Ribonuclease-Mediated Control of Body Fat Article

Ribonuclease-Mediated Control of Body Fat. *Dev. Cell* **39**, 359–369 (2016).

124. Slobin, L. The role of eucaryotic elongation factor Tu in protein synthesis. *Eur. J. Biochem.* **563**, 555–563 (1980).
125. Truitt, M. L. *et al.* Differential Requirements for eIF4E Dose in Normal Development and Cancer. *Cell* **162**, 59–71 (2015).
126. Sonenberg, N. & Hinnebusch, A. G. Regulation of Translation Initiation in Eukaryotes: Mechanisms and Biological Targets. *Cell* **136**, 731–745 (2009).
127. Furic, L. *et al.* EIF4E phosphorylation promotes tumorigenesis and is associated with prostate cancer progression. *Proc. Natl. Acad. Sci. U. S. A.* **107**, 14134–14139 (2010).
128. Rosenwald, I. B., Rhoads, D. B., Callanan, L. D., Isselbacher, K. J. & Schmidt, E. V. Increased expression of eukaryotic translation initiation factors eIF-4E and eIF-2α in response to growth induction by c-myc. *Proc. Natl. Acad. Sci. U. S. A.* **90**, 6175–6178 (1993).
129. Leclercq, T. M., Moretti, P. A. B. & Pitson, S. M. Guanine nucleotides regulate sphingosine kinase 1 activation by eukaryotic elongation factor 1A and provide a mechanism for eEF1A-associated oncogenesis. *Oncogene* **30**, 372–378 (2011).
130. Losada, A. *et al.* Binding of eEF1A2 to the RNA-dependent protein kinase PKR modulates its activity and promotes tumour cell survival. *Br. J. Cancer* **119**, 1410–1420 (2018).
131. Laham-Karam, N., Pinto, G. P., Poso, A. & Kokkonen, P. Transcription and Translation Inhibitors in Cancer Treatment. *Front. Chem.* **8**, 1–24 (2020).
132. Zou, Z., Tao, T., Li, H. & Zhu, X. mTOR signaling pathway and mTOR inhibitors in cancer: Progress and challenges. *Cell Biosci.* **10**, 1–11 (2020).
133. Tao, Z. *et al.* Autophagy suppresses self-renewal ability and tumorigenicity of glioma-initiating cells and promotes Notch1 degradation. *Cell Death Dis.* **9**, (2018).
134. Stein, K. C., Morales-Polanco, F., van der Lienden, J., Rainbolt, T. K. & Frydman, J. Ageing exacerbates ribosome pausing to disrupt cotranslational proteostasis. *Nature* **601**, 637–642 (2022).
135. Gerashchenko, M. V., Peterfi, Z., Yim, S. H. & Gladyshev, V. N. Translation elongation rate varies among organs and decreases with age. *Nucleic Acids Res.* **49**, E9 (2021).

136. Webster, G. C. & Webster, S. L. Decline in synthesis of elongation factor one (EF-1) precedes the decreased synthesis of total protein in aging Drosophila melanogaster. *Mech. Ageing Dev.* **22**, (1983).
137. Varshavsky, A. N-degron and C-degron pathways of protein degradation. *Proc. Natl. Acad. Sci. U. S. A.* **116**, 358–366 (2019).
138. Bonsignore, L. A. *et al.* NRMT1 knockout mice exhibit phenotypes associated with impaired DNA repair and premature aging. *Mech. Ageing Dev.* **146**–**148**, 42–52 (2015).
139. Anderson, R. M., Bitterman, K. J., Wood, J. G., Medvedik, O. & Sinclair, D. A. Nicatinamide and PNC1 govern lifespan extension by calorie restriction in Saccharomyces cerevisiae. *Nature* **423**, 181–185 (2003).
140. Liu, Y. & Chang, A. Heat shock response relieves ER stress. *EMBO J.* **27**, 1049–1059 (2008).
141. Lithgow, G. J., White, T. M., Hinerfeld, D. A. & Johnson, T. E. Thermotolerance of a Long-lived Mutant of Caenorhabditis elegans. *J. Gerontol.* **49**, 270–276 (1994).
142. Johnson, T. E. *et al.* Longevity genes in the nematode Caenorhabditis elegans also mediate increased resistance to stress and prevent disease. *J. Inherit. Metab. Dis.* **25**, 197–206 (2002).
143. Park, S., Tedesco, P. M. & Johnson, T. E. Oxidative stress and longevity in Caenorhabditis elegans as mediated by SKN-1. *Aging Cell* **8**, 258–269 (2009).
144. Morgan, C. T., Lee, M. H. & Kimble, J. Chemical reprogramming of Caenorhabditis elegans germ cell fate. *Nat. Chem. Biol.* **6**, 102–104 (2010).
145. Cha, D. S., Datla, U. S., Hollis, S. E., Kimble, J. & Lee, M. H. The Ras-ERK MAPK regulatory network controls dedifferentiation in Caenorhabditis elegans germline. *Biochim. Biophys. Acta - Mol. Cell Res.* **1823**, 1847–1855 (2012).
146. O'Reilly, L. P., Luke, C. J., Perlmutter, D. H., Silverman, G. A. & Pak, S. C. C. elegans in high-throughput drug discovery. *Adv. Drug Deliv. Rev.* **69**–**70**, 247–253 (2014).
147. Kobet, R. A. *et al.* Caenorhabditis elegans: A model system for anti-cancer drug discovery and therapeutic target identification. *Biomol. Ther.* **22**, 371–383 (2014).